Finanziato dall'Unione europea
NextGenerationEU

Ministero dell'Università e della Ricerca

Italiadomani
PIANO NAZIONALE DI RIPRESA E RESILIENZA

TOR VERGATA
UNIVERSITÀ DEGLI STUDI DI ROMA

Quantum Noise and Optical Aberration Control

Lorenzo Aiello

Tor Vergata University of Rome
INFN Rome Tor Vergata

ET Technology School – Cagliari (Italy)
December 13th, 2024

Einstein Telescope Infrastructure Consortium (ETIC - IR0000004)
PNRR MISSIONE 4, COMPONENTE 2, INVESTIMENTO 3.1
http://www.einstein-telescope.it

Outline

- Introduction: noises, sensitivity curve, quantum noise
- The problem: thermal effects and optical aberrations
- The (current) solution: the Thermal Compensation System (TCS)
- The (future) solution: TCS upgrades in view of ET-HF

Introduction

Noises, sensitivity curve, quantum noise

Gravitational Waves in a nutshell

- Ripples in the fabric of the spacetime
- Propagating at the speed of light
- Solution of Einstein’s equations
- Two polarization states

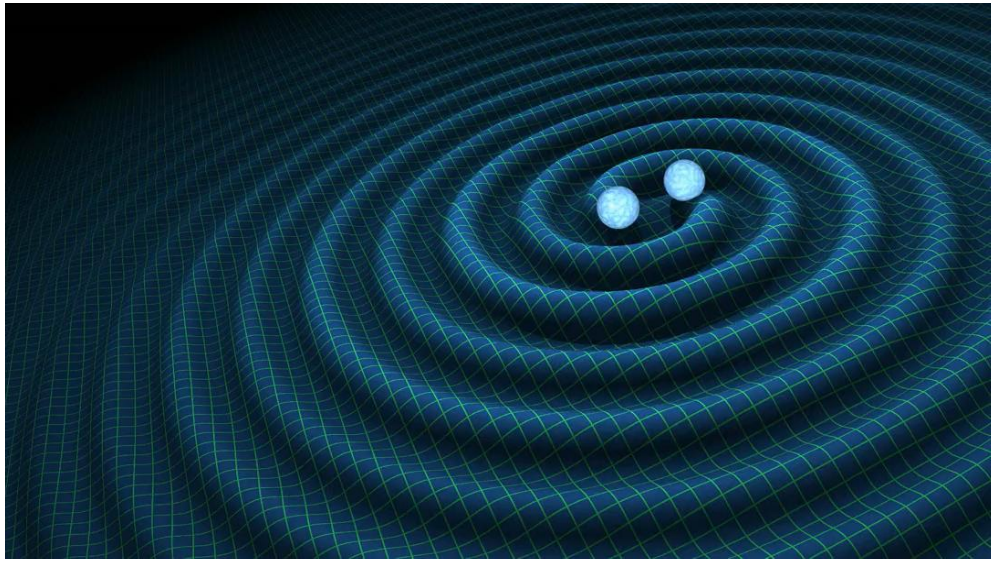

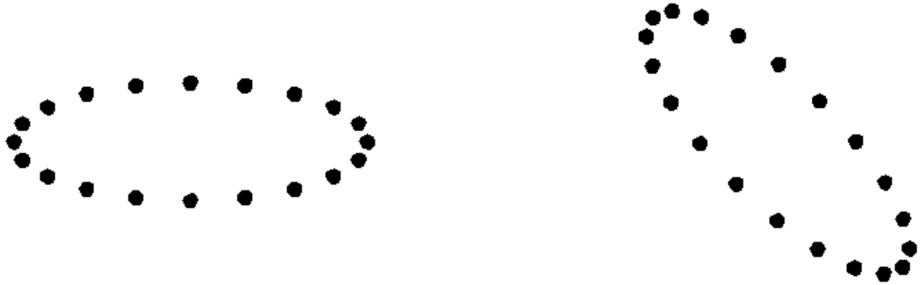

Key for detection: interference

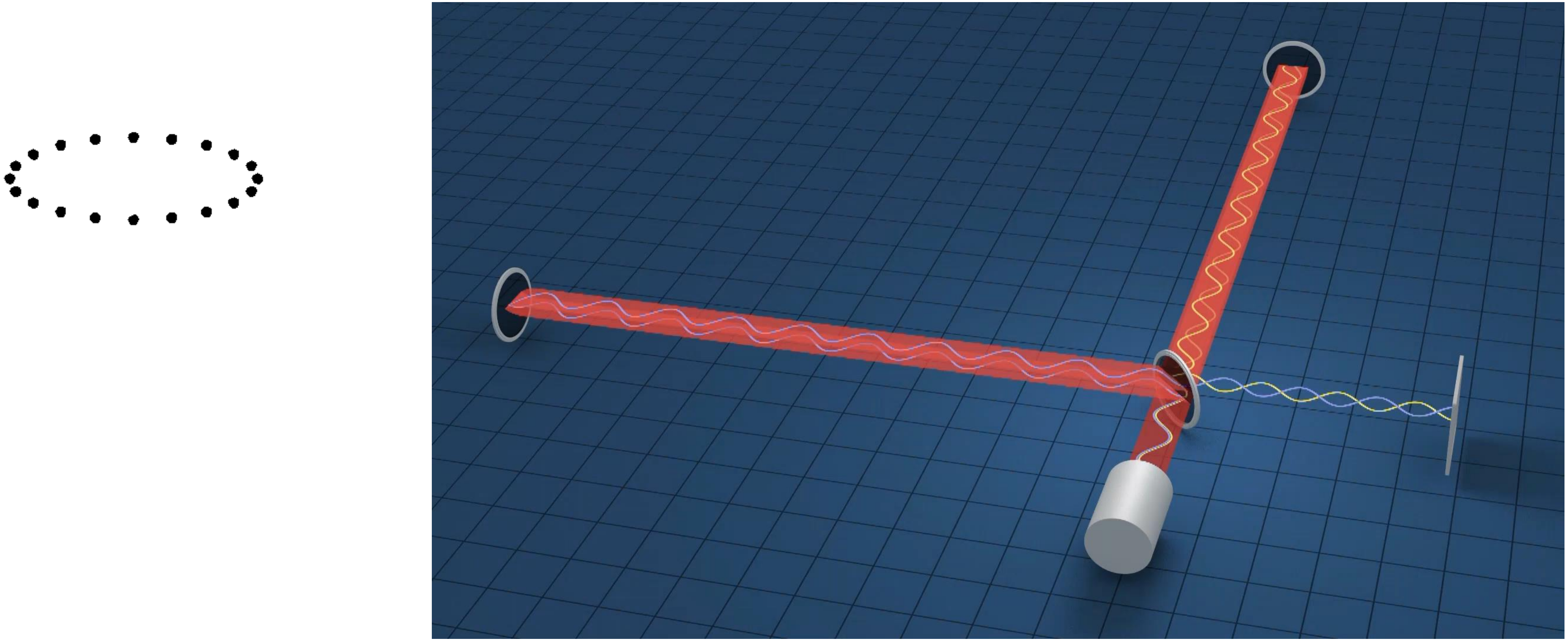

Strain sensitivity and sensitivity curve

$$\left.\begin{array}{l}\text{Arm length } L\sim 10^{3}\ m\\[2ex] \text{GW amplitude } h\sim 10^{-21}\\[2ex] \text{Arm length change } \Delta L=\dfrac{1}{2}hL\end{array}\right\}\Delta L\sim 10^{-18}\ m$$

Sensitivity curves shows usually show the strain sensitivity

$$h=2\frac{\Delta L}{L}$$

Advanced Virgo plus theoretical sensitivity curve (P_{in}= 40 W)

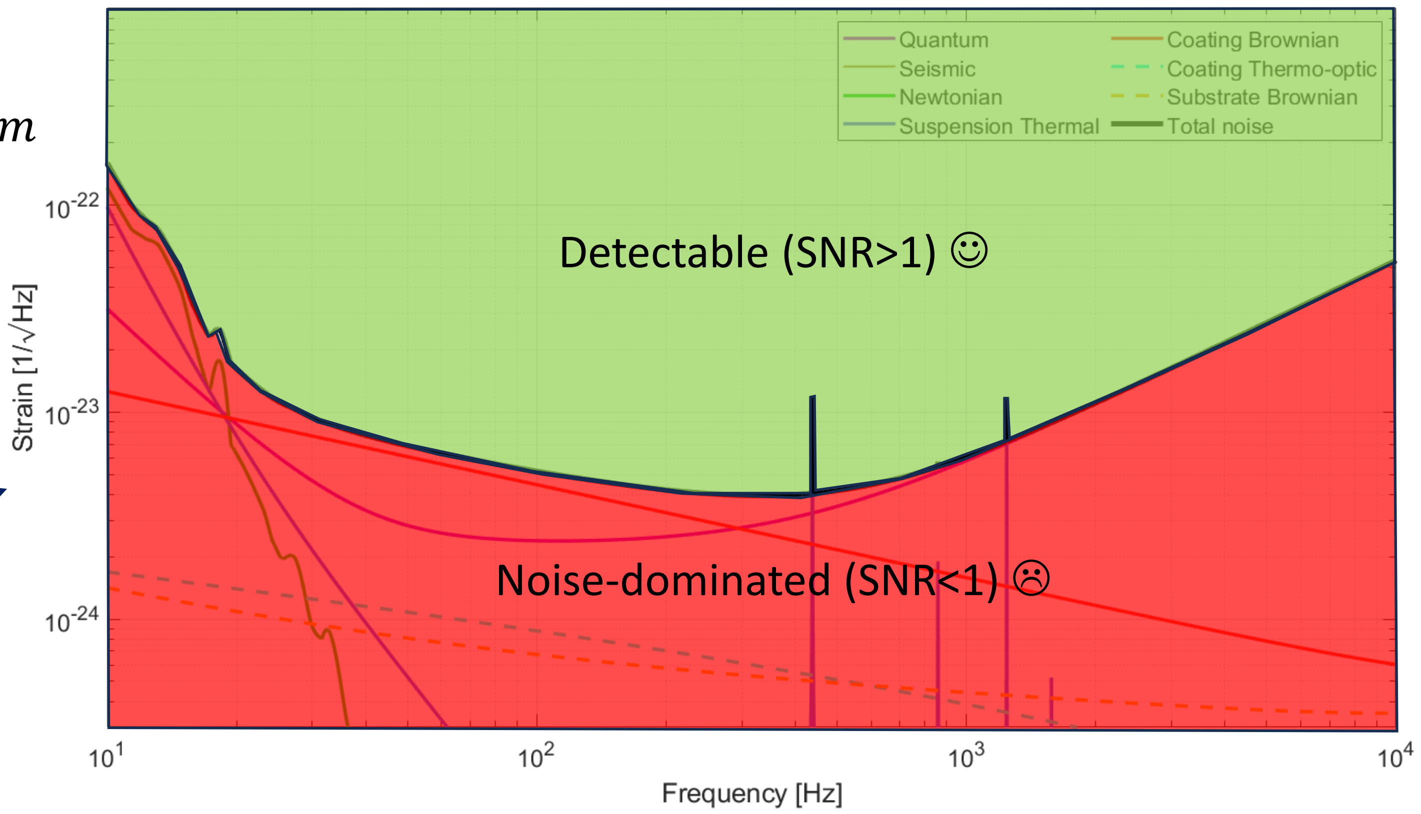

Sensitivity curve – Limiting noises

Sum of fundamental and technical noises

- **Seismic/Newtonian noise < 20 Hz**
- **Thermal noise ~ 20 - 300 Hz**
- **Quantum (Shot) noise > 300 Hz**

Advanced Virgo plus theoretical sensitivity curve (P_{in}= 40 W)

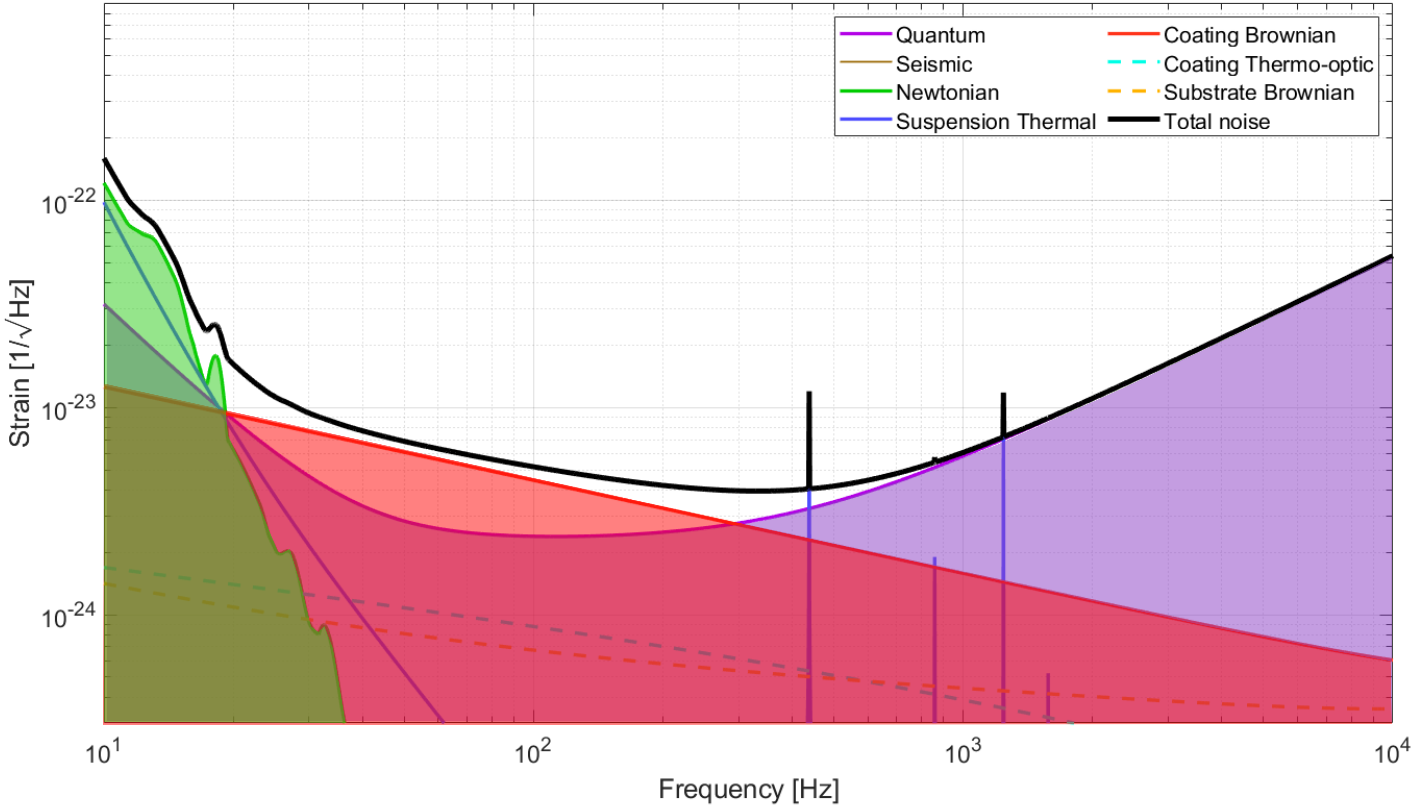

ET sensitivity curves

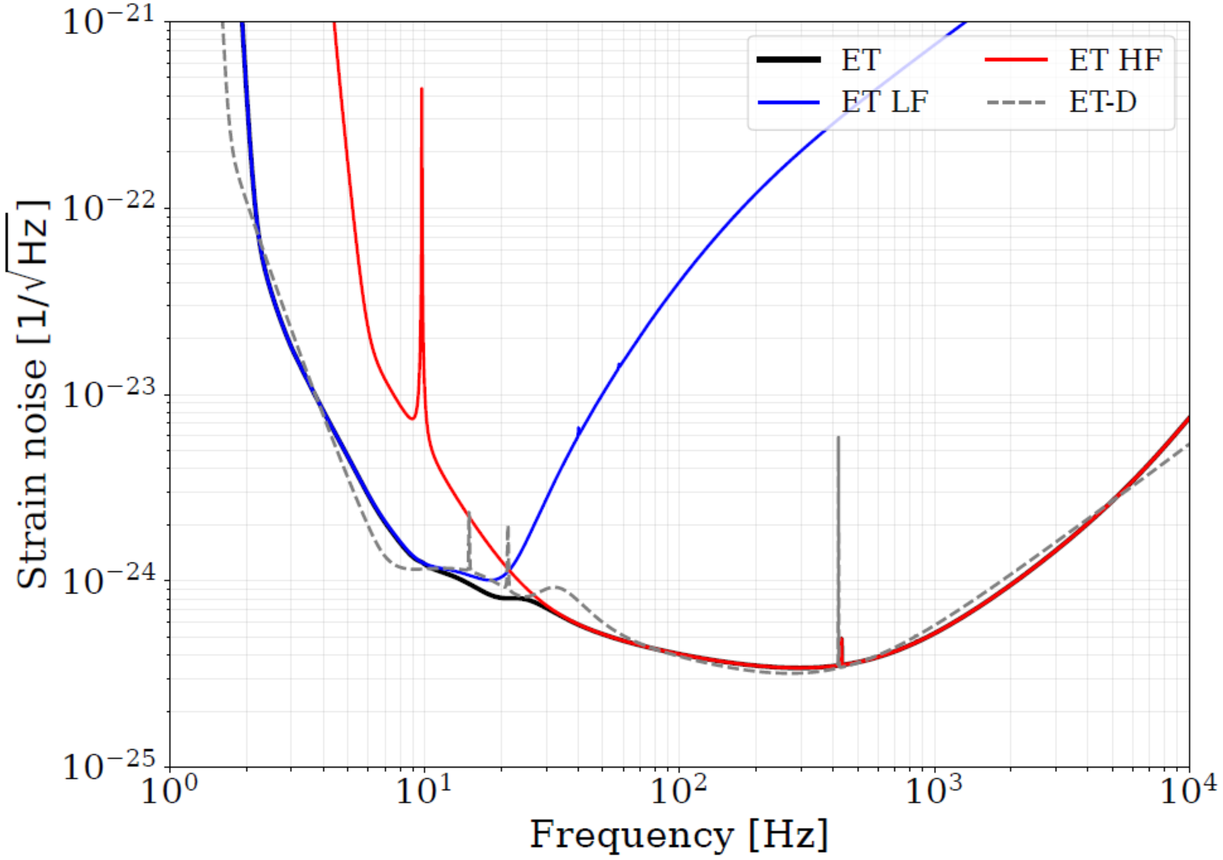

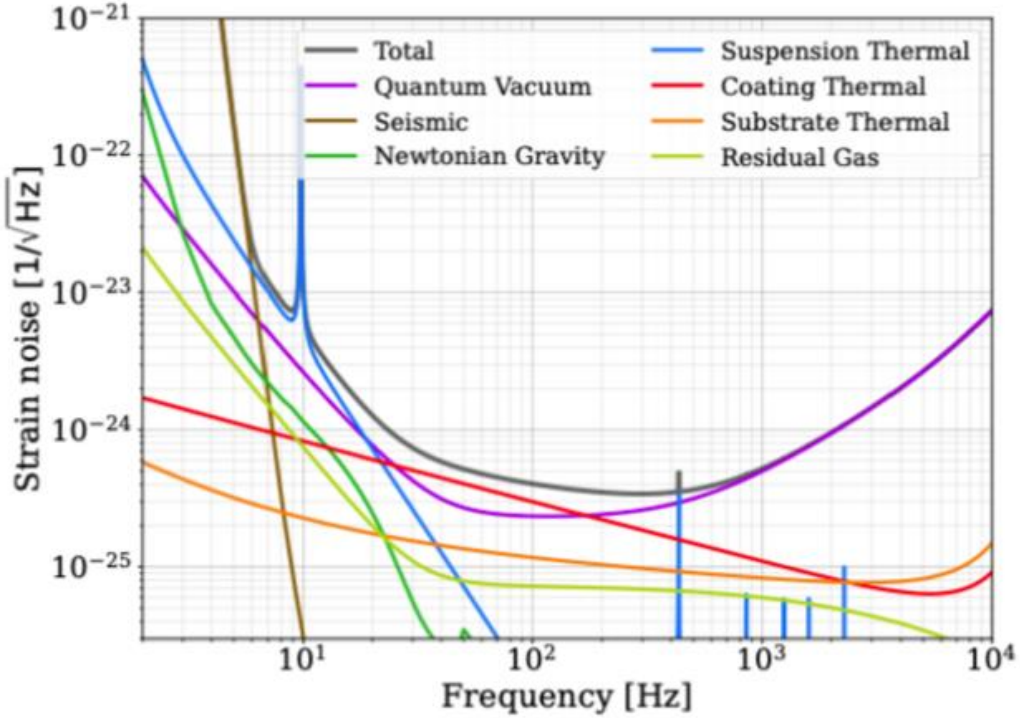

Figure 1: Strain noise budget of the HF detector.

Quantum electromagnetic field review

$a, a^\dagger$: quantum mechanical complex-amplitude operators

- If we consider a single mode of the electromagnetic field, we can write the electric field as

$$E(t) = C(ae^{-i\omega t} + a^\dagger e^{-i\omega t})$$

$$a = X_1 + iX_2$$

X_1 and X_2 are Hermitian operators giving the dimensionless amplitudes for the mode's two quadrature phases →

$$E(t) = \frac{C}{2}(X_1\cos(\omega t) + X_2\sin(\omega t))$$

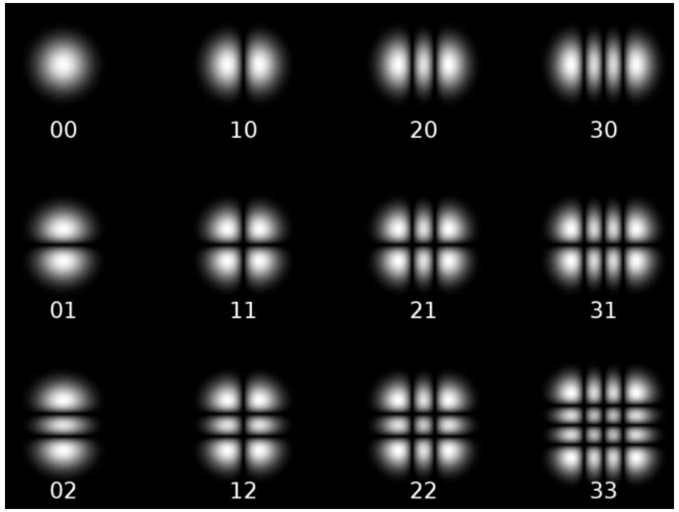

- Due to the Heisenberg's uncertainty principle, for the uncertainties of the **quadrature**'s it holds

$$\boxed{\Delta X_1 \Delta X_2 \geq \frac{1}{4}}$$

Phase space representation of (coherent) states

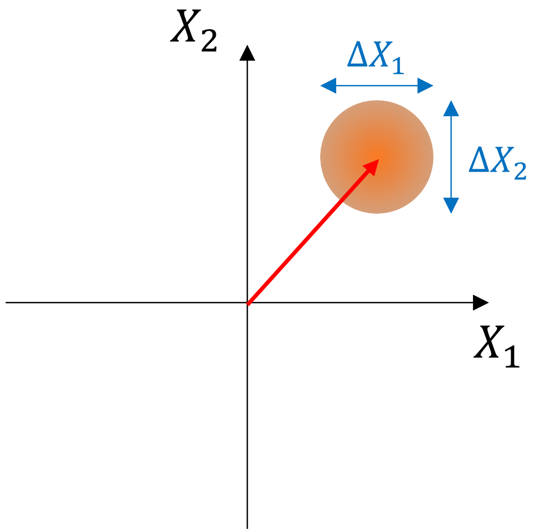

Phase space representation of a generic coherent state with a phasor 'stick' and quadrature uncertainty 'ball', centred at $\alpha = X_1 + \mathrm{i}X_2$.

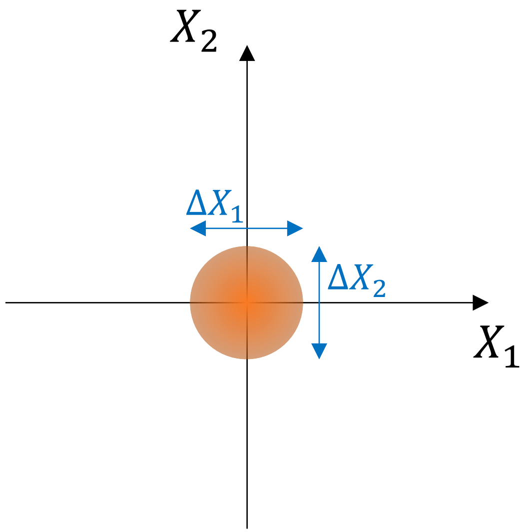

Phase space representation of a vacuum coherent state.

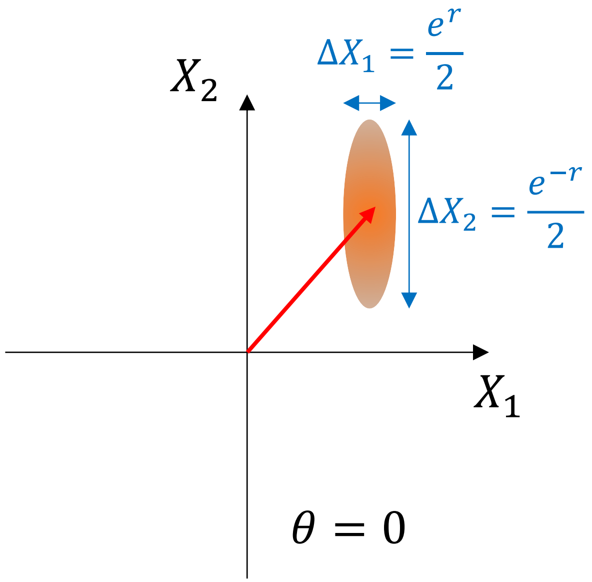

Phase-squeezed coherent state.

Quantum noise

- Quantum noise is due to the quantum fluctuations of the vacuum - the ground state of the electromagnetic field.
- This state has fluctuations, which enter in the interferometer from the output port.

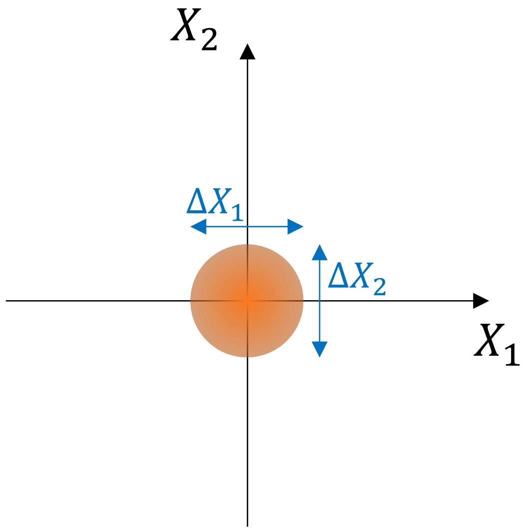

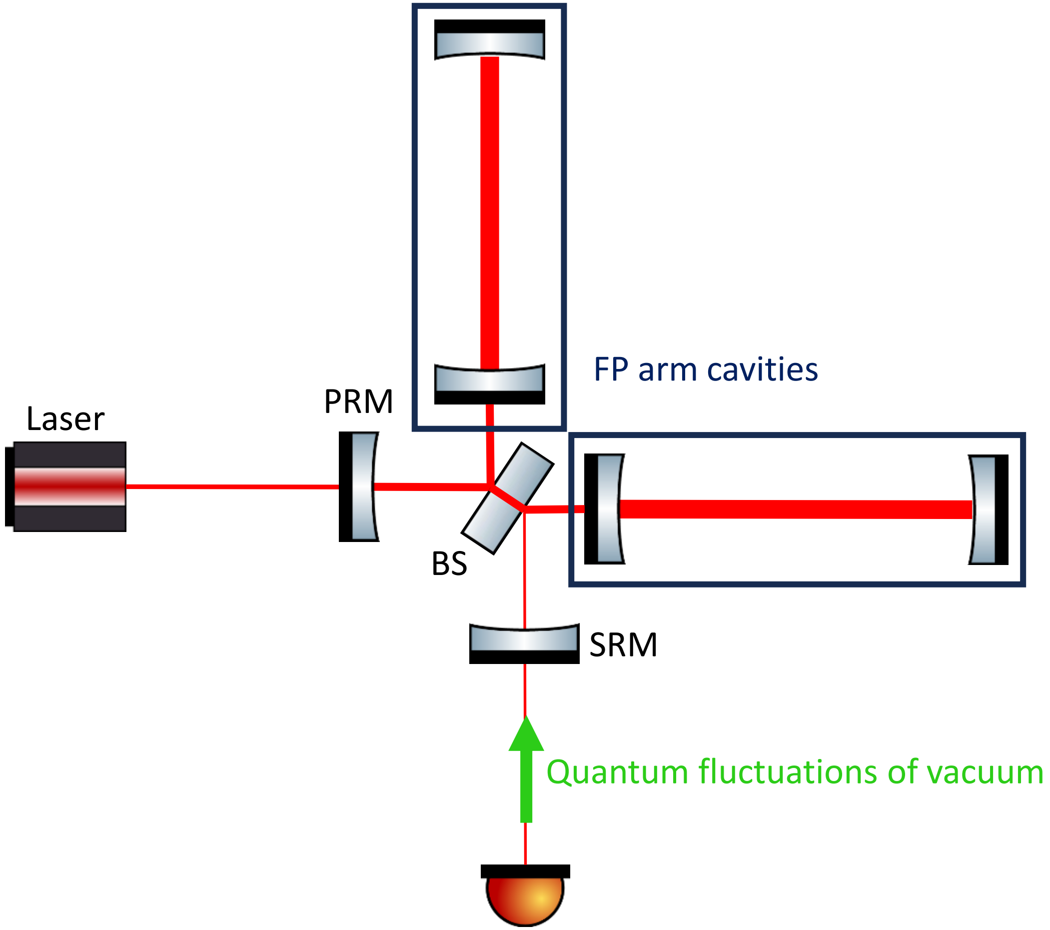

Quantum noise

- This state has fluctuations, which enter in the interferometer from the output port and when superposed on the input laser light, they produce two effects.

- Uncertainty on the number of output photons, which produces a fluctuation in the intensity at the photodetector and then on the measured power.

Quantum shot noise

- A beam of photons that impinges on a mirror and is reflected back exerts a pressure on the mirror itself. Since the number of photons arriving on the mirror fluctuates, the pressure fluctuates too and generates a stochastic force that shakes the mirrors.

Quantum radiation pressure noise

Quantum noise components (or "quadratures")

This phenomenon is one of the reasons why ET employs two interferometers to maintain high sensitivity in as wide a frequency range as possible.

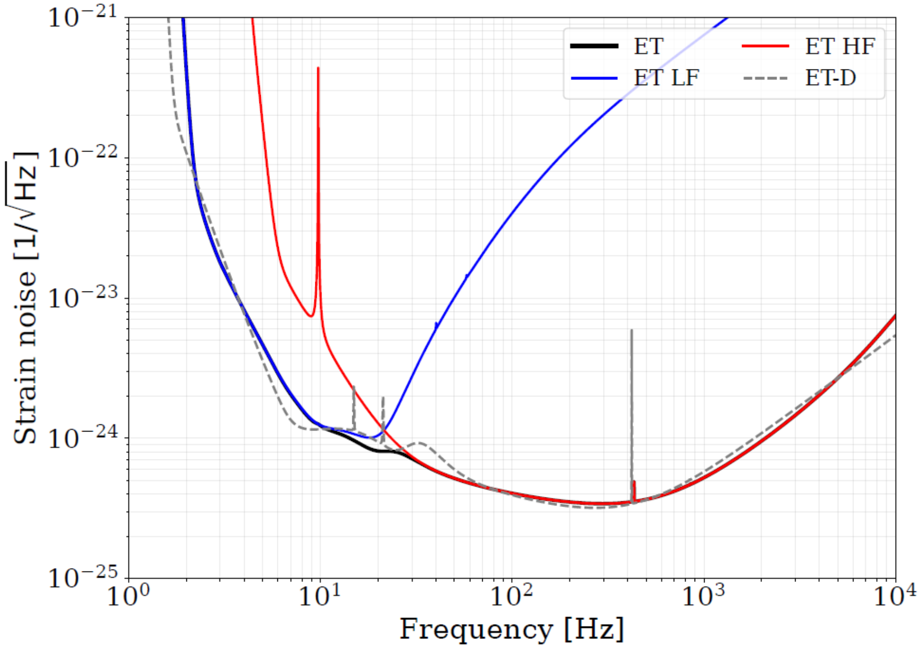

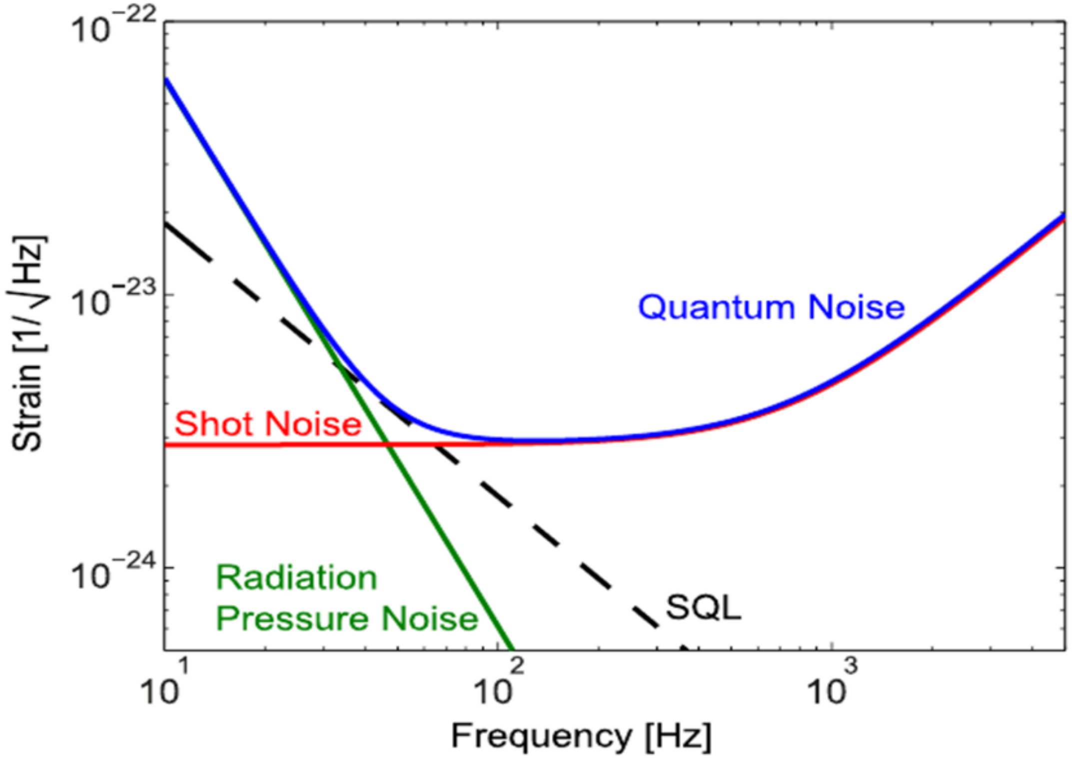

Quantum shot noise

- Uncertainty/fluctuations in the measured power

With no GW: $\Delta P_{shot} = \sqrt{\frac{\hbar \omega_L P_0}{T}}\, sin(\varphi_0)$

With GW: $\Delta P_{GW} = \frac{P_0}{2} |sin(2\varphi_0)| \frac{4\pi L h_0}{\lambda_L}$

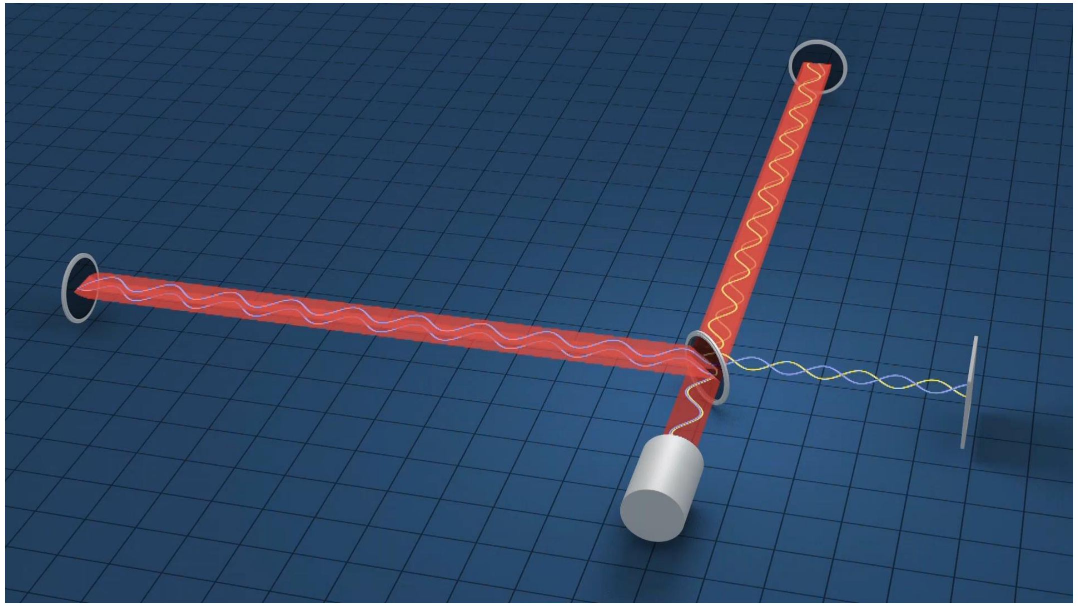

P_0: input power

λ_L, ω_L: laser wavelength and angular frequency

L: interferometer arms' length

h_0: GW amplitude

$\hbar$: reduced Planck constant

T: observation time

φ_0: interferometer working point (dark fringe, half fringe, etc.)

Quantum shot noise

- What we want is the SNR: $\frac{S}{N} = \frac{\Delta P_{GW}}{\Delta P_{shot}}$
- Only-shot-noise approximation, and assuming optimal orientation:

$$S_n^{\frac{1}{2}}(f)|_{shot} = \frac{\lambda_L}{4\pi L}\sqrt{\frac{2\hbar\omega_L}{\enclose{circle}{P_0}}}$$

- $\sqrt{S_n(f)}$: *spectral strain sensitivity* or *spectral amplitude*

$$\left[\sqrt{S_n(f)}\right] = \frac{1}{\sqrt{Hz}}$$

- <u>Key point: the power is at the denominator</u>
- <u>To reduce shot noise contribution, input (and then circulating) power must be increased</u>

Quantum shot noise and radiation pressure

$S_n^{\frac{1}{2}}(f)|_{shot} \propto \sqrt{\frac{1}{P_0}}$ → To reduce shot noise contribution, increase P_0

↓

Beam of photons exerts a pressure on the mirror itself

← N° of photons fluctuates as $\sqrt{N_\gamma}$

↓

Radiation pressure fluctuates ↔ Stochastic force shakes the mirror

↓

Stochastic force grows as $\sqrt{P_0}$

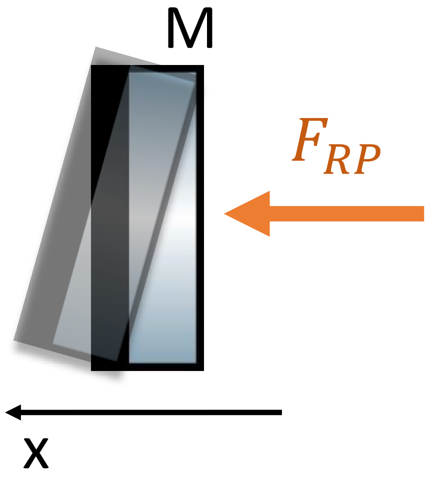

Quantum shot noise and radiation pressure

Power increase: good

Power increase: not good

$$S_n^{\frac{1}{2}}(f)|_{shot} \propto \sqrt{\frac{1}{P_0}}$$

Stochastic force grows as $\sqrt{P_0}$

Beyond a certain limit, fluctuations in radiation pressure will become important and will dominate over the shot noise…

… but this is not an issue for ET-HF

The Standard Quantum Limit

- Increasing the input power, more photons impinge on the photodetector. The signal-to-shot-noise ratio increases but at the same time the force exerted on the mirrors increases as well, resulting in a larger radiation pressure noise.

- The total quantum noise is the sum in quadrature of these two components. Because the Heisenberg's minimal uncertainty relation holds, one noise will be reduced at the expense of increasing the other one.

- This defines a lower limit that apparently cannot be surpassed, i.e. the *Standard Quantum Limit* (SQL).

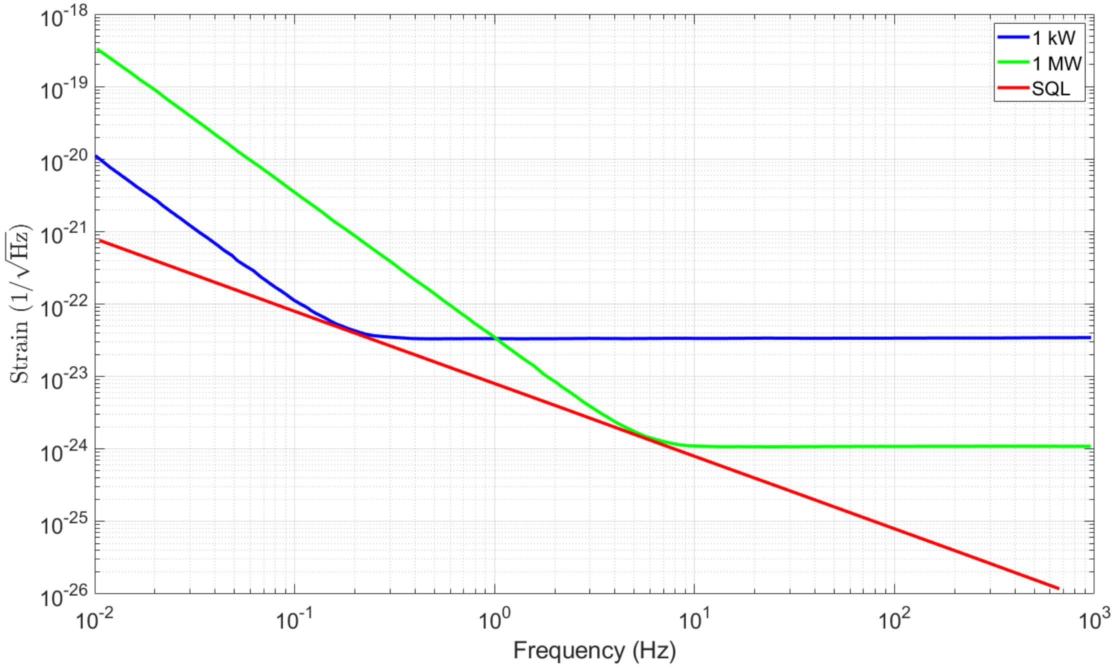

$$S_n(f)|_{opt} = S_n(f)|_{shot} + S_n(f)|_{rad\,pres}$$

Optical read-out noise

The road towards high-power operations

- Increasing the power will reduce shot noise contribution, at the expense of increasing radiation pressure (which is currently not a limiting noise in Advanced Virgo plus, nor it will be in ET-HF).
- To get closer to the expected ET-HF power, in the next years/Observing Runs a step-by-step increase of the power is foreseen in Advanced Virgo plus and in the subsequent Virgo_nEXT project.

	O4	**O5**	**Post-O5**	**Third generation**
Parameter	**Current Advanced Virgo plus**	**Advanced Virgo plus best**	**Virgo_nEXT best**	**ET High-Frequency**
Injected power	18 W	125 W	277 W	500 W
Arm power	~100 kW	390 kW	1.5 MW	3 MW

Current estimates

- <u>However, the power increase and the subsequent improvement in the signal-to-shot-noise ratio does not come for free…</u>

The problem

Thermal effects and optical aberrations

Wavefront

- The wavefront of a time-varying wave field is the set of all points having the same phase.

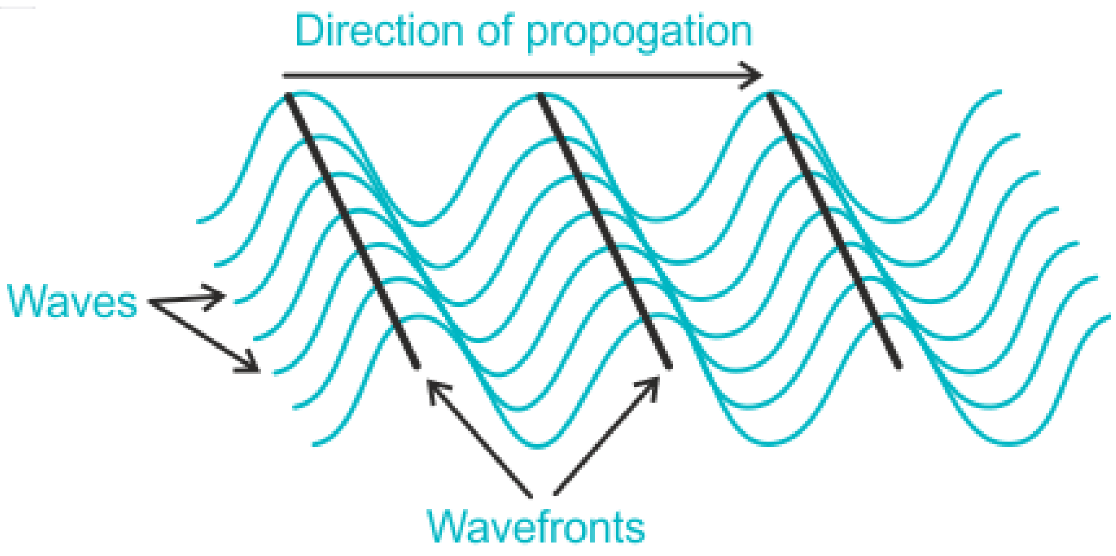

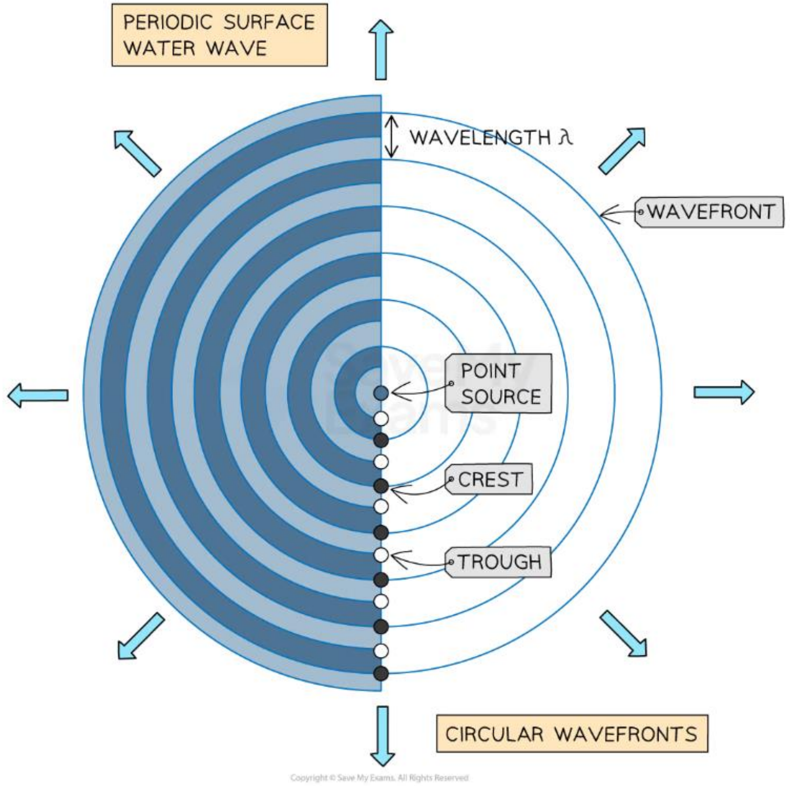

Copyright © Save My Exams. All Rights Reserved

Wavefront

- Waves can be represented graphically in two different ways:
    - **Wavefronts** - lines joining all the points that oscillate **in phase** and are perpendicular to the direction of motion (and energy transfer)
    - **Rays** - lines showing the direction of motion (and energy transfer) of the wave perpendicular to the wavefront

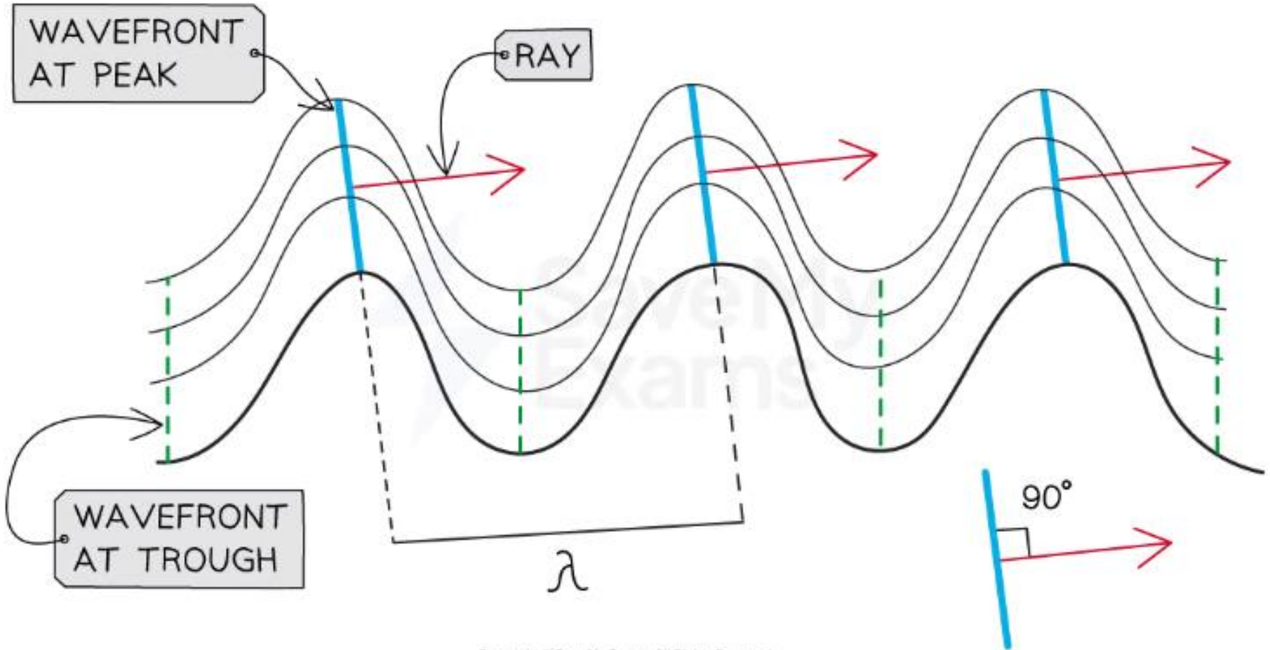

Copyright © Save My Exams. All Rights Reserved

Wavefront distortions

- A Wavefront Distortion (WD) is defined as any transverse or spatial variation from the nominal one in the surface of equal phase (wavefront) of an electromagnetic field accumulated after reflection from or transmission through an optical element.

- Laser light used in the GW interferometers is an electromagnetic field behaving exactly in this way when it encounters a non-perfect mirror.

Wavefront distortions

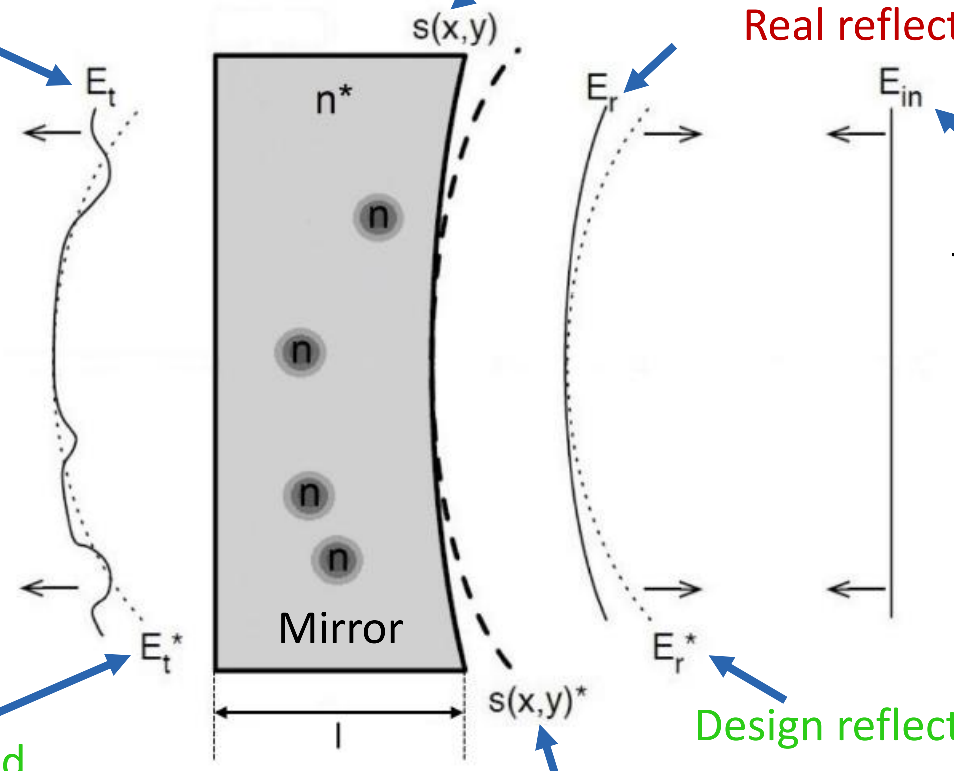

Real transmitted field

Mirror real curvature

Real reflected field real

Incident field

--- Design values

— Real values

Design transmitted field

Design reflected field

Mirror design curvature

Wavefront distortions in reflection

$$\Delta WD_r(x,y) = s^*(x,y) - s(x,y)$$

Wavefront distortions in transmission

$$\Delta WD_t(x,y) = \int_0^l [n(x,y,z) - n^*]\, dz$$

Parenthesis: core optics in a GW detector

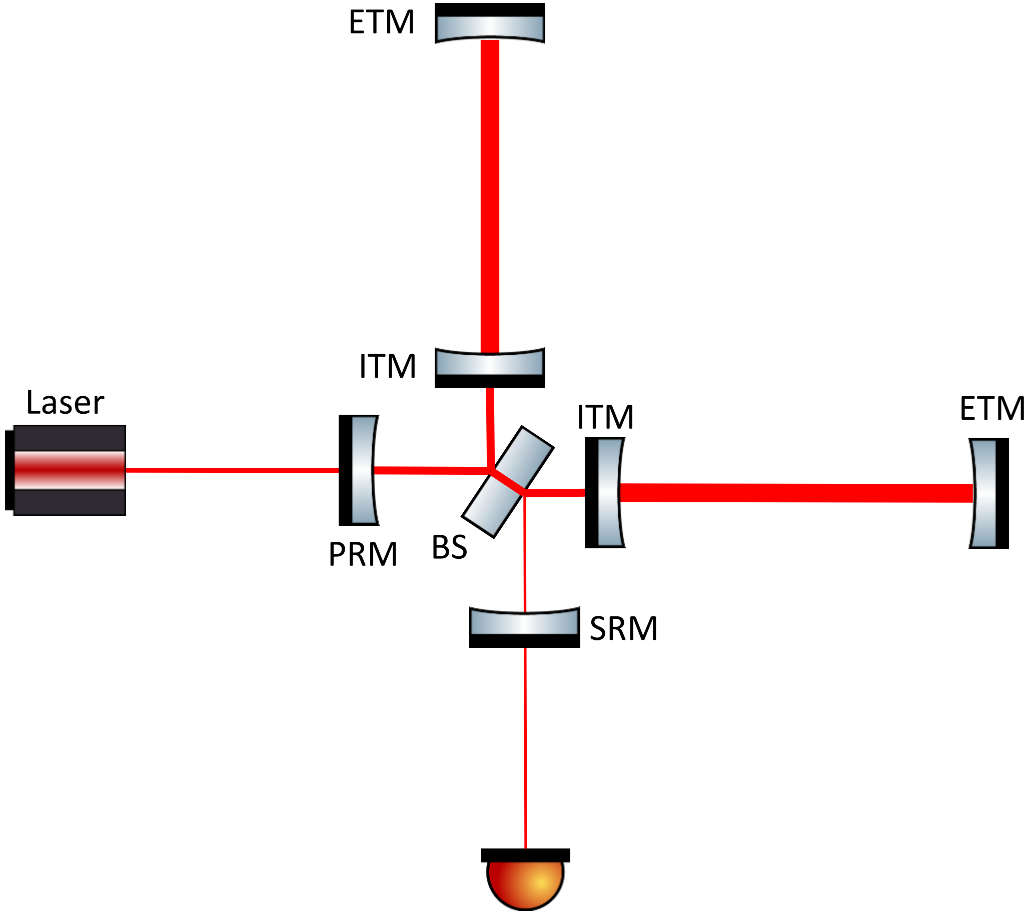

- PRM: Power-Recycling Mirror
- SRM: Signal-Recycling Mirror
- BS: Beamsplitter
- ITM: Input Test Mass
- ETM: End Test Mass

Parenthesis: core optics in a GW detector

- High-purity fused silica substrate
- Diameter 35 cm, mass ~ 40 kg
- Radius of Curvature (RoC) ~1.5 km
- Produced by ZYGO (USA)
- Multi-layer coating made of amorphous oxides deposited on the surfaces of the mirrors to make them High Reflective (HR) or Anti Reflective (AR)
- Power absorption of about ~ 0.5 ppm

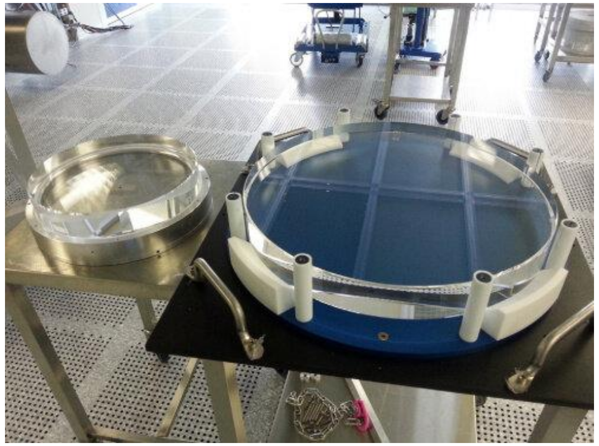

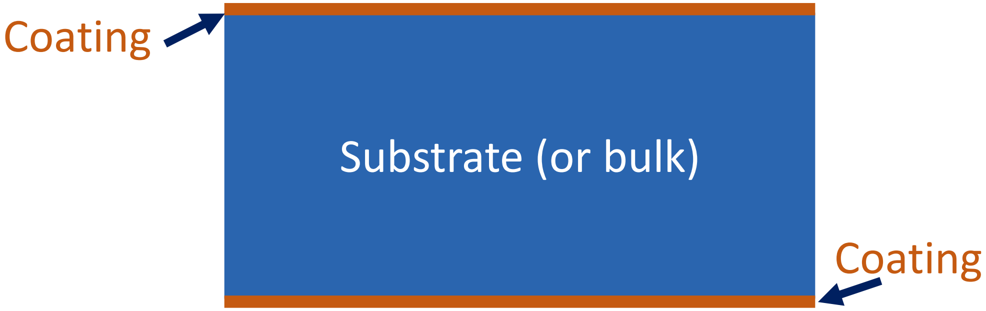

Mirror components' representation (not in scale!)

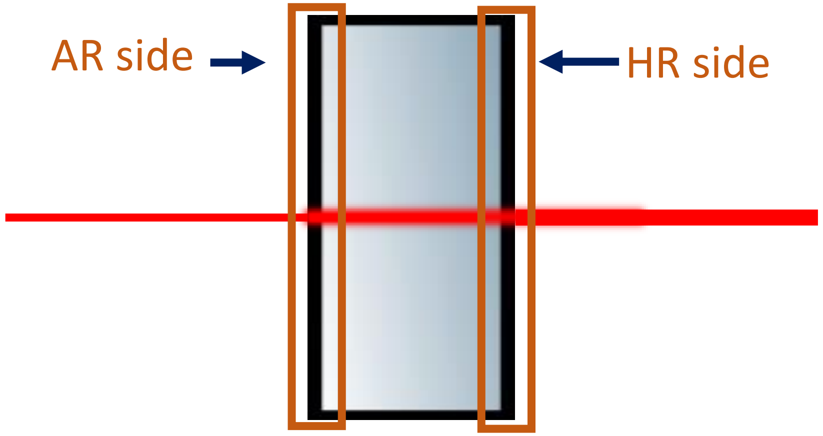

Parenthesis: core optics in a GW detector

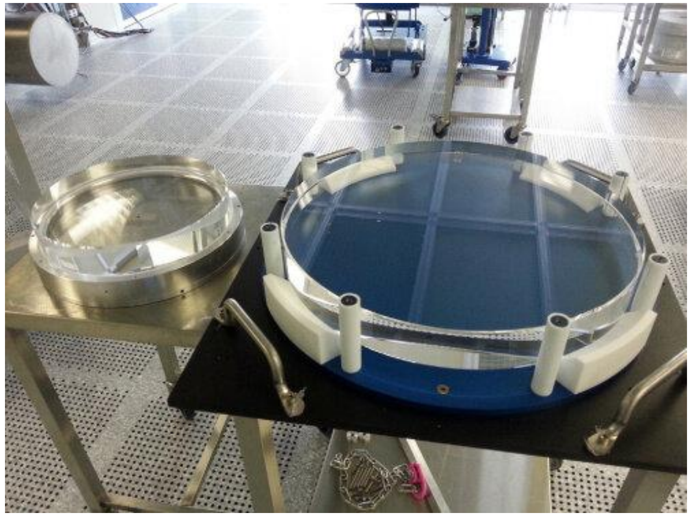

Mirror production and polishing

Integration in the payload

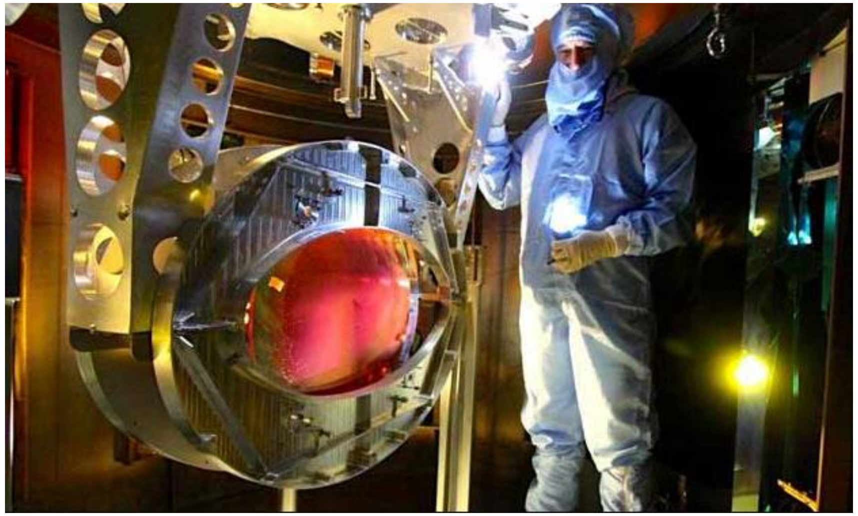

Integration in the interferometer

Sources of optical aberrations

Two classes of sources

Imperfections in the production process of the mirrors

Cold defects

Absorption of optical power in the coatings and substrates of the optics

Thermal effects

Cold defects

Each optic has its own cold defects map which represents the residual imperfections due to the production processes such as :

- non-uniformities in the substrate
- surface figure errors
- inhomogeneity of refractive index
- impurities
- manufacturing errors (e.g., Radius of Curvatures (RoC) mismatches)

The cold RoCs are different from the design ones

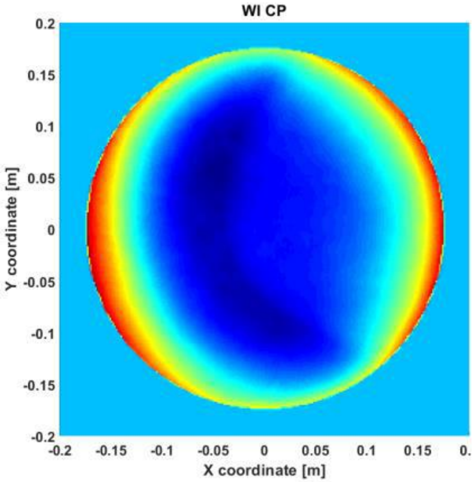

Diverging not-symmetric lens

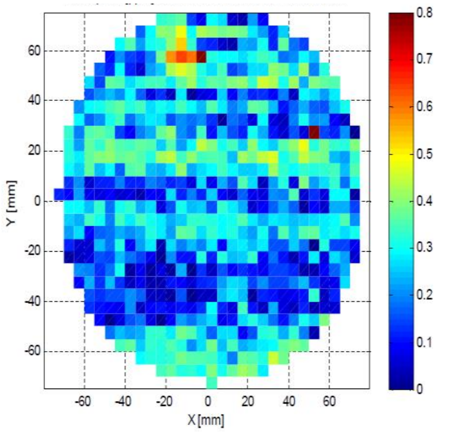

Not-uniform absorption

Optic	Nominal RoC	Real RoC
PRM	1430 m	1477 m
SRM	1430 m	1440 m
ITM	1420 m	1426 m
ETM	1683 m	1696 m

Thermal effects

- For an optic with thickness *l* and refractive index *n*, the Optical Path Length (OPL) inside it is defined as

$$OPL = n \cdot l$$

- Due to the absorption - in the coatings and substrates - of a fraction of the laser power, the optic increases its temperature and expands, changing the OPL inside it through three different mechanisms:

  - thermal lensing (or thermo-optic effect)

  - thermo-elastic deformation

  - elasto-optic effect

Thermal effects

- **Thermal lensing**: OPL distortions due to the dependence of the refractive index from temperature variation

$$\Delta OPL_T = \frac{dn}{dT}\int_0^h \Delta T\, ds$$

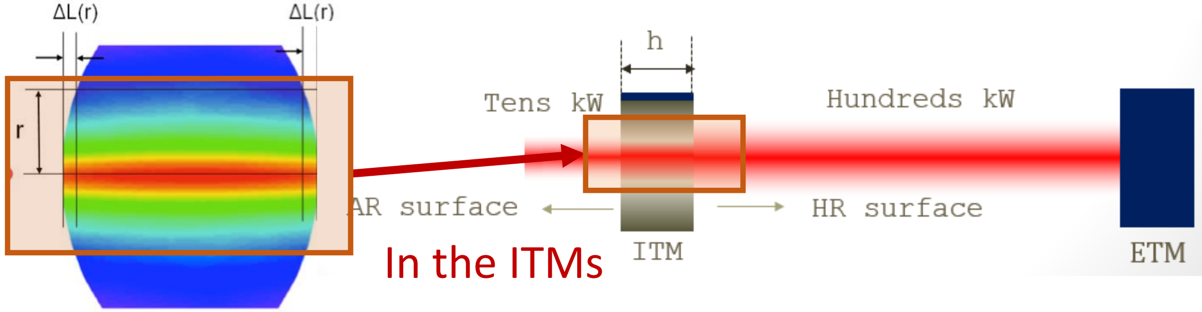

In the ITMs

- **Thermo-elastic deformation** ($\alpha \neq 0$): change of RoC of mirrors due to the absorption of laser power

$$\underbrace{\Delta OPL_T \approx \alpha(1+\sigma)(n-1)\int_0^h \Delta T\, dz}_{\text{Effect in transmission}} \qquad \underbrace{\Delta OPL_R \approx 2\alpha\int_0^h \Delta T\, dz}_{\text{Effect in reflection}}$$

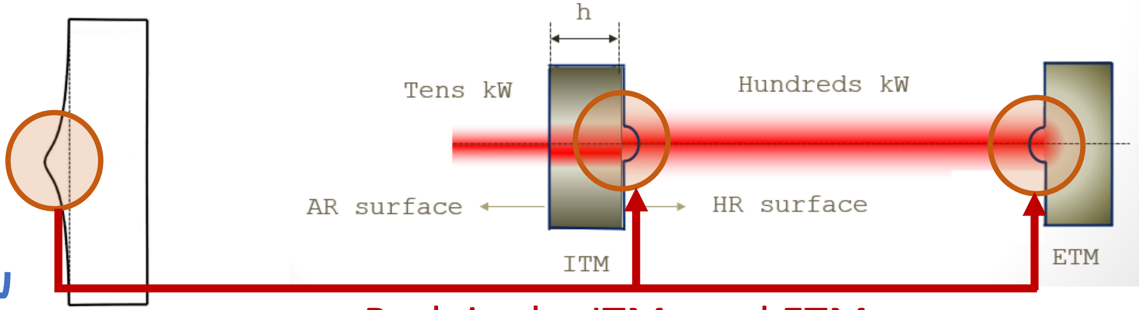

Both in the ITMs and ETMs

- **Elasto-optic effect** (usually negligible): due to the local refractive index change for the mechanical strain caused by the thermal expansion

$$\Delta OPL = \int_0^h \Delta n_{EO}\, dz \approx -\alpha p_{11}\int_0^h \Delta T\, dz$$

Optical aberrations

- In optics, aberration is a property of optical systems that causes light to be spread out over some region of space rather than focused to a point.
- Aberrations cause the image formed by an optical system to be blurred or distorted, with the nature of the distortion depending on the type of aberration.
- Aberration can be defined as a departure of the performance of an optical system from the predictions of paraxial optics.

- Optical aberrations are usually expressed by the **double-indexes Zernike polynomials**

$$Z_n^m(\rho, \theta)$$

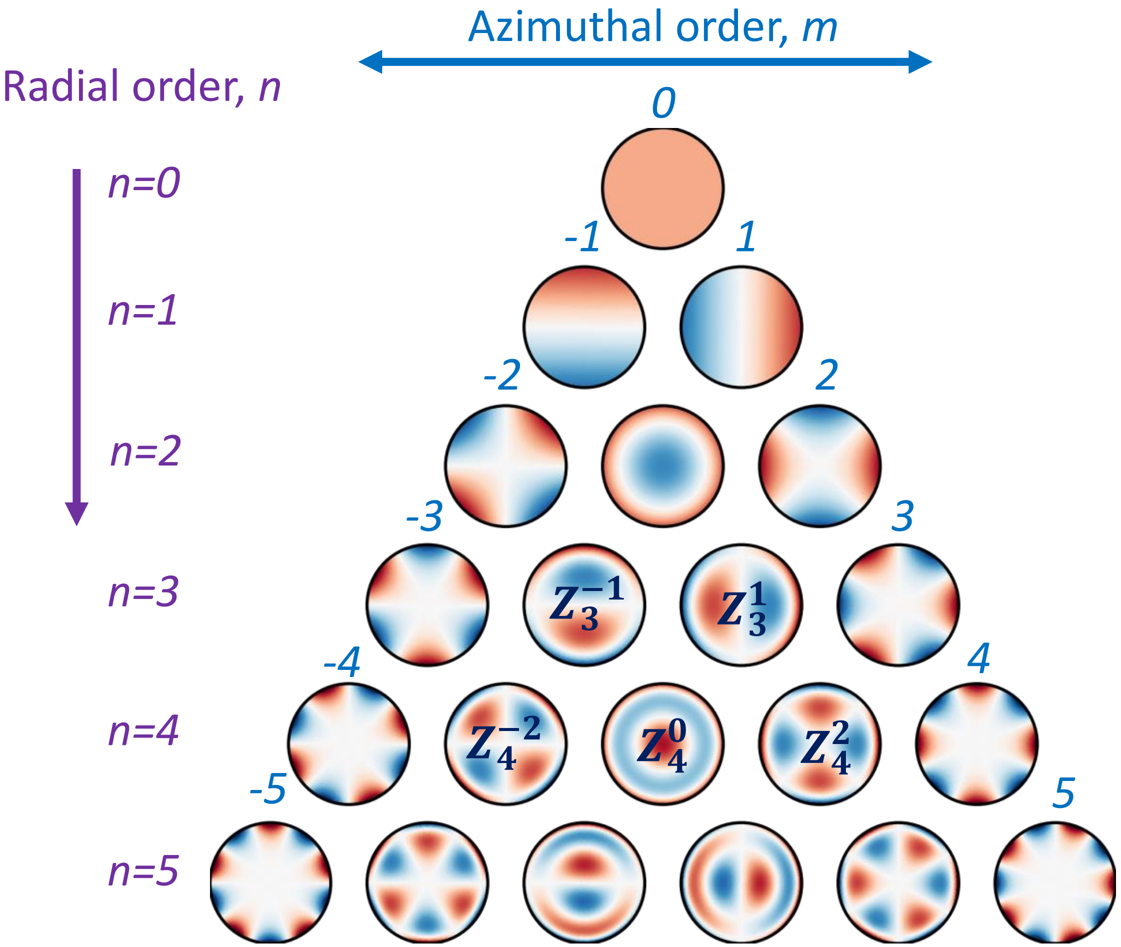

Zernike polynomials

- Sometimes Zernike polynomials with a single index *j* are used. The conversion between the indexes is shown in the following table.

	m=-3	m=-2	m=-1	m=0	m=1	m=2	m=3
n=0				j=0			
n=1			j=1		j=2		
n=2		j=3		j=4		j=5	
n=3	j=6		j=7		j=8		j=9

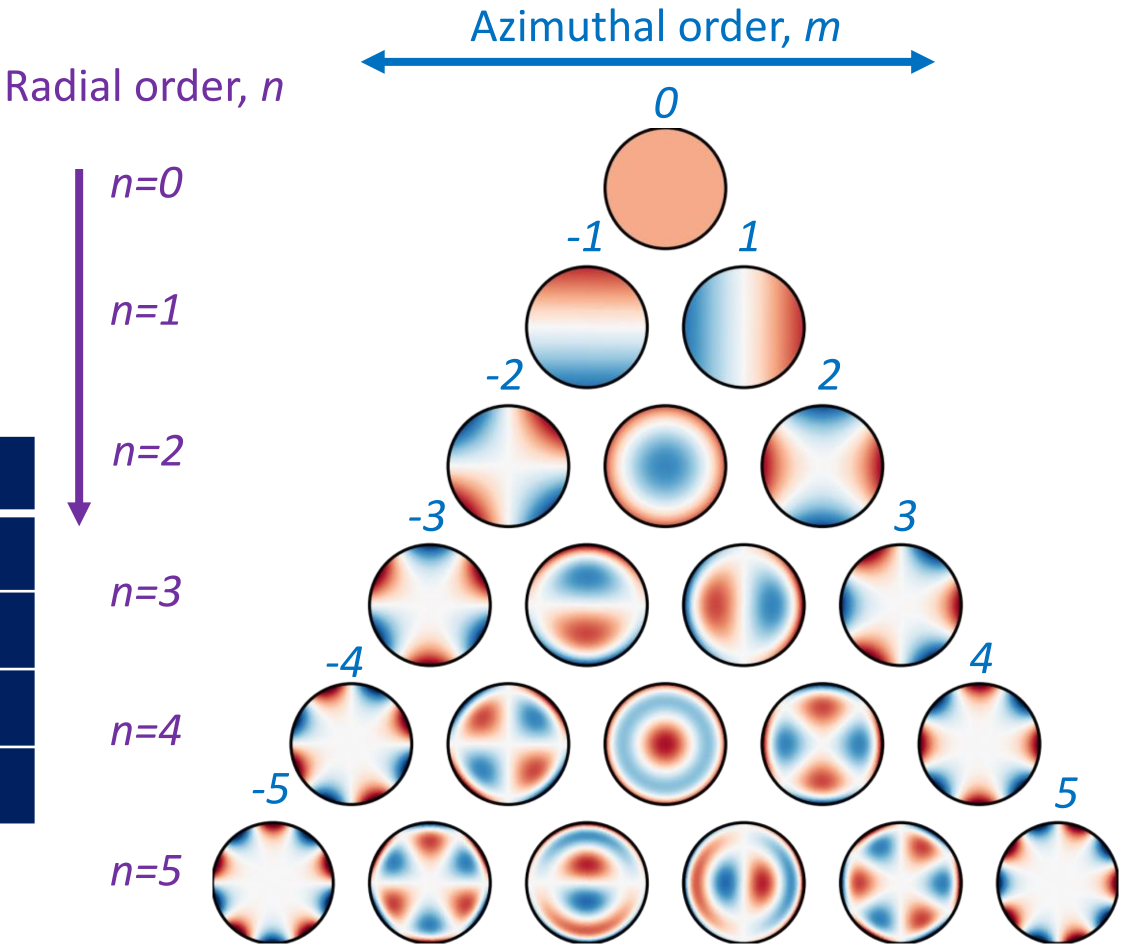

Finanziato dall'Unione europea NextGenerationEU
Ministero dell'Università e della Ricerca
Italiadomani PIANO NAZIONALE DI RIPRESA E RESILIENZA
TOR VERGATA UNIVERSITÀ DEGLI STUDI DI ROMA

Most common aberrations

j	n	m	Z_n^m	Meaning
0	0	0	Z_0^0	Piston (constant term)
1	1	-1	Z_1^{-1}	Tilt in y-direction
2	1	1	Z_1^1	Tilt in x-direction
3	2	-2	Z_2^{-2}	Astigmatism with axis ±45°
4	2	0	Z_2^0	Field curvature, defocus
5	2	2	Z_2^2	Astigmatism with axis at 0° or 90°

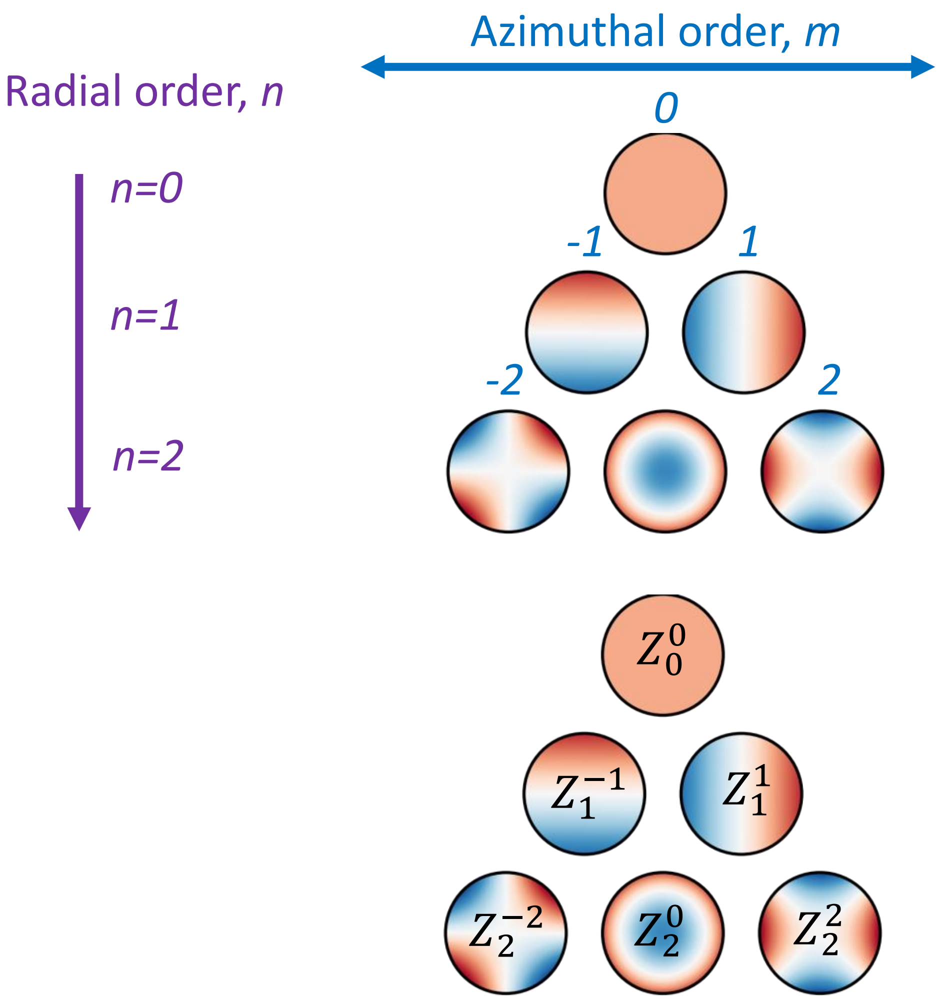

Piston and tilt

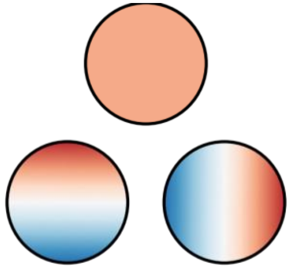

- **Piston** is the mean value of a wavefront. The piston coefficient is typically expressed in wavelengths of light at a particular wavelength.
- **Tilt** is a deviation in the direction a beam of light propagates. Tilt quantifies the average slope in both the X and Y directions of a wavefront.
- Piston and tilt are not actually true optical aberrations, as they do not represent or model curvature in the wavefront. Defocus is the lowest order true optical aberration. If piston and tilt are subtracted from an otherwise perfect wavefront, a perfect, aberration-free image is formed.

Field curvature aberration

- Field curvature arises due to the curved optics surfaces. It causes the image to lie on a surface that is not a plane.
- Unfortunately, the image plane is typically a flat CCD or CMOS image sensor and so whilst the field curvature doesn't blur the image on the curved image surface, it does result in blurring on the planar image surface.
- Because parallel rays do not focus on a plane - but rather on a curved surface – this causes radial defocusing, i.e. for a given sensor position, only a circular crown will be in focus.

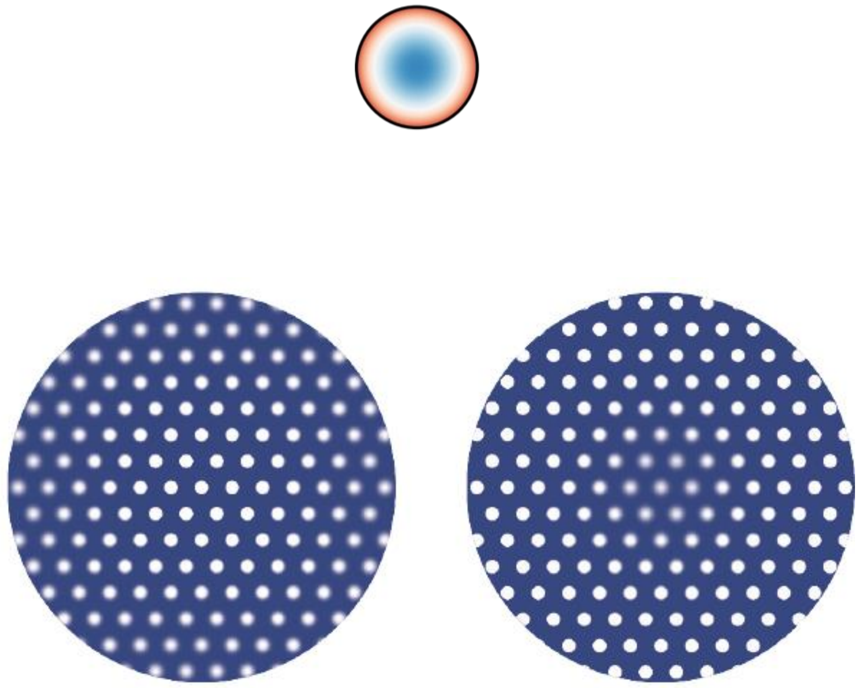

How thermal effects affect a GW interferometer

- Thermal effects change the detector optical configuration from the design one.

- The effects of the wavefront distortions on the detector performances are divided in three categories:
  <u>1) Increase of noise at the output port due to WD in the arms of the interferometer.</u>
  These effects lead to:
  a) reduction in the power at the BS (and then the shot noise increases);
  b) increase of the power leaking out of the output port (adding shot noise to the measurement).

  <u>2) Reduction of the GW signal amplification</u>

  <u>3) Interferometer stability and robustness reduction</u>

Therefore, thermal effects (and the optical aberrations generated by them) must be properly **compensated**…

The (current) solution

Sensing and correcting the WDs: the Thermal Compensation System

Aberrations' sensing: Hartmann Wavefront Sensor

- To directly measure the thermally-induced wavefront variation on each mirror a dedicated sensor, the Hartmann Wavefront Sensor (HWS) is engaged.

- The HWS is made by a Charge Coupled Device (CCD), an opaque plate containing an array of apertures known as Hartmann Plate (HP), two fins used to dissipate the heat of the CCD and two slabs of copper to carry the heat from the CCD to the fins.

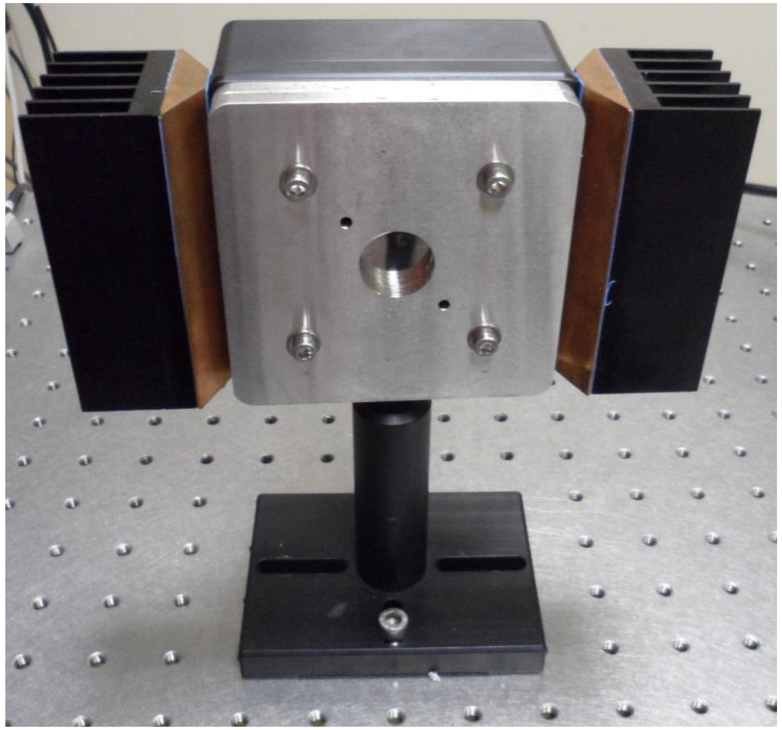

Hartmann Wavefront Sensor

- HWS is a differential sensor, i.e. it computes the difference between a wavefront acquired at time t with a reference one.
- A probe beam is used to detect the aberration, which is produced by a Superluminescent Light Emitting Diode (SLED). The probe beam impinges on the mirror under test through a dedicated optical setup that will be described in detail later.
- Once arrived on the mirror, the SLED beam is reflected back on the same path and it impinges on the HP.

- The HWS has to detect:

- the OPL increase due to the **thermal lensing** in the two ITMs (***on-axis measurements***)
- the **thermo-elastic deformation** of the HR surfaces of all the test masses (***off-axis measurements***).

Hartmann Wavefront Sensor – On-axis and off-axis setup

- To sense the aberrations in a wide area around the optical axis, an afocal telescope is used to increase the size of the probe beam on the mirror surface.

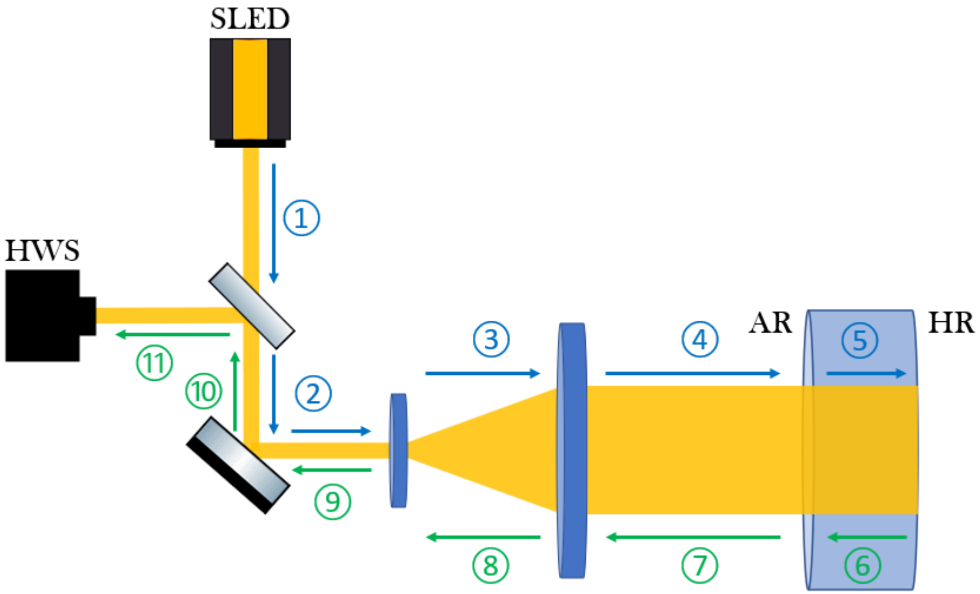

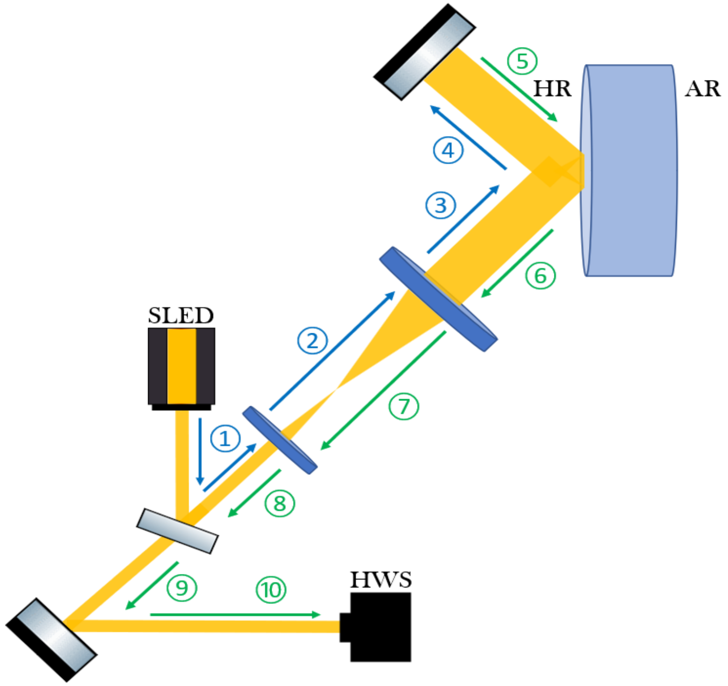

The **on-axis measurements** are carried on by the HWSs in transmission to monitor the **thermal lens** effect in the Input mirrors of the Fabry–Pérot arm cavities.

The **off-axis measurements** are taken by the HWSs in reflection to detect the **thermoelastic deformation** in both Input and End mirrors of the Fabry-Pérot arm cavities.

Hartmann Wavefront Sensor – Working principle

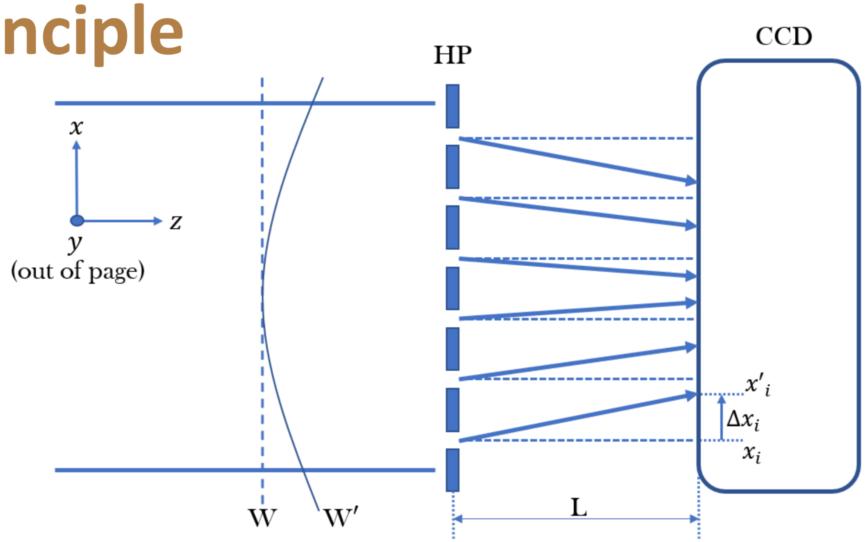

- When an aberrated wavefront W’ pass through the HP, a set of rays travels a distance L (lever arm) and form a CCD a pattern on light spots recorded as digital image.
- The position x_i of the *i-th* spot is determined by a centroid algorithm and then the displacement Δx_i of each spot from a previously measured reference position x_i is evaluated. In the end the data set of all spots measurement gives the gradient of the wavefront change ΔW

$$\frac{\partial \Delta W}{\partial x} = \frac{\Delta x_i}{L}$$

- The wavefront change ΔW is computed by integrating the discrete gradient field.

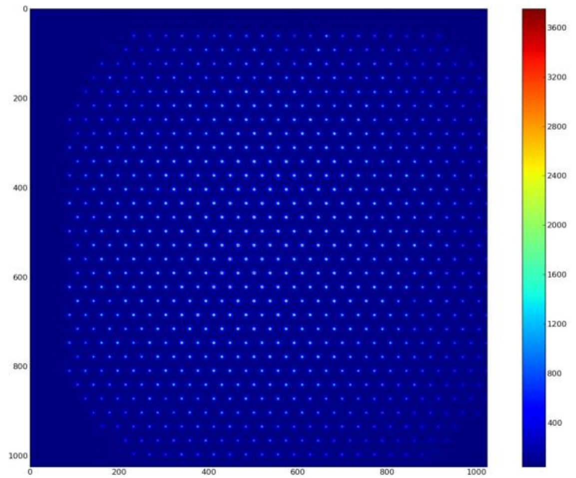

Phase camera

- The Phase Camera (PC), developed by the Nikhef group, is a sensor able to measure the amplitude and phase maps of the electromagnetic fields in the interferometer and produces relative maps.

- PC is a complementary sensor to the above-described HWS, with the difference that it takes global measurements, i.e. it cannot distinguish between the different optics.

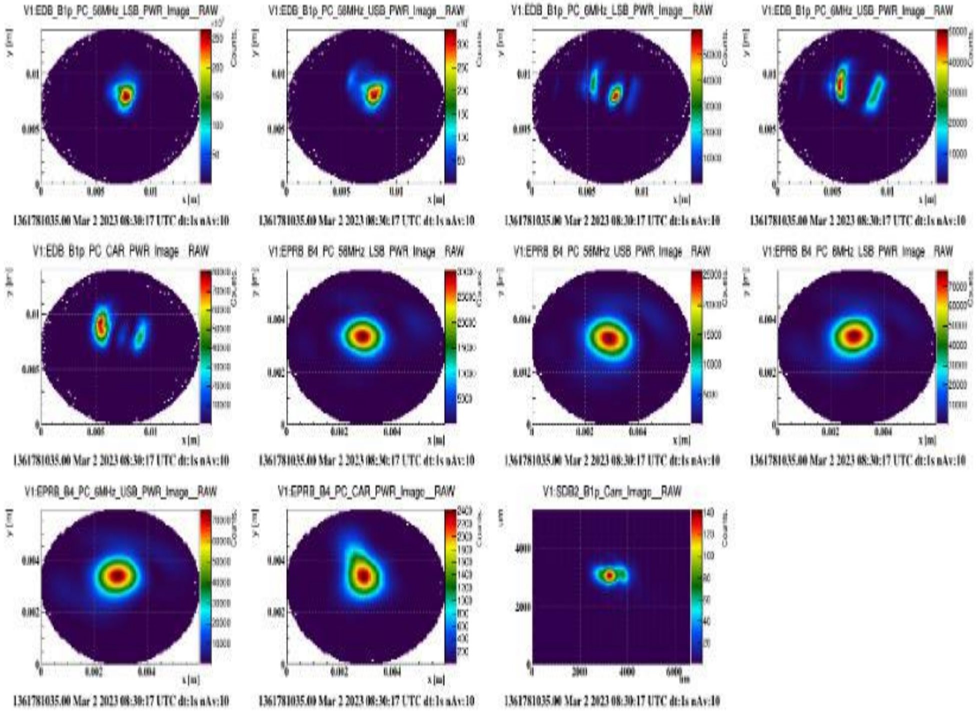

Correction of the thermo-elastic deformation

- The thermo-elastic deformation creates a bump in the centre of the mirrors, changing their RoC from the design value.
- A value of RoC far from the design one compromises the correct working of the detector, because it reduces the fraction of the laser fundamental mode circulating in the cavity by scattering the power in HOMs, therefore generating unwanted effects.

Correction strategy

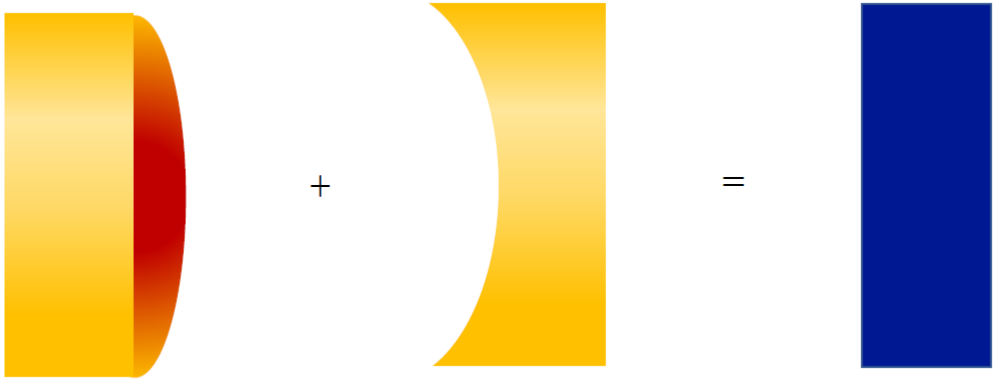

Bump due to the power absorption

Mirror heated by TCS actuator

Cold mirror

Fundamental mode

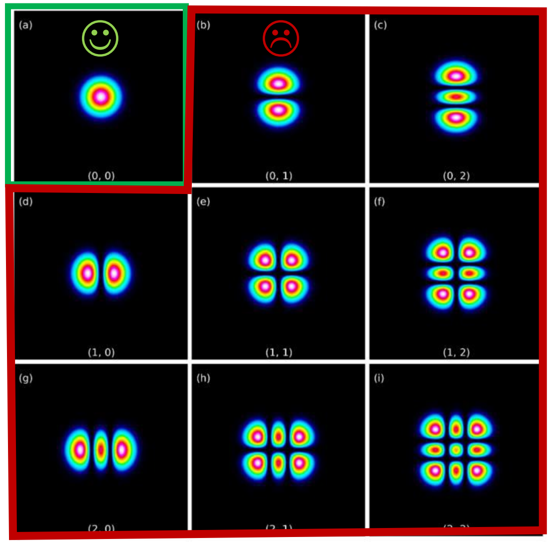

Higher order modes (HOMs)

Correction of the thermo-elastic deformation: Ring Heater

- The chosen device devoted to the compensation of this effect is an adaptive optical actuator called Ring Heater (RH). It allows also to compensate static curvature errors due to an incorrect manufacturing or polishing.

- The RH is composed of two heaters and a shield. Each heater consists of a coil of Nickel Chrome wires wrapped around a ring of pyrex. The wires are heated via the Joule effect and the high emissivity of the pyrex assures an effective radiation of power.

- The RH is mechanically-centred around all optics within 0.5 cm, which allows users to easily identify the centre of the related Test Mass (TM) on the HWS maps.

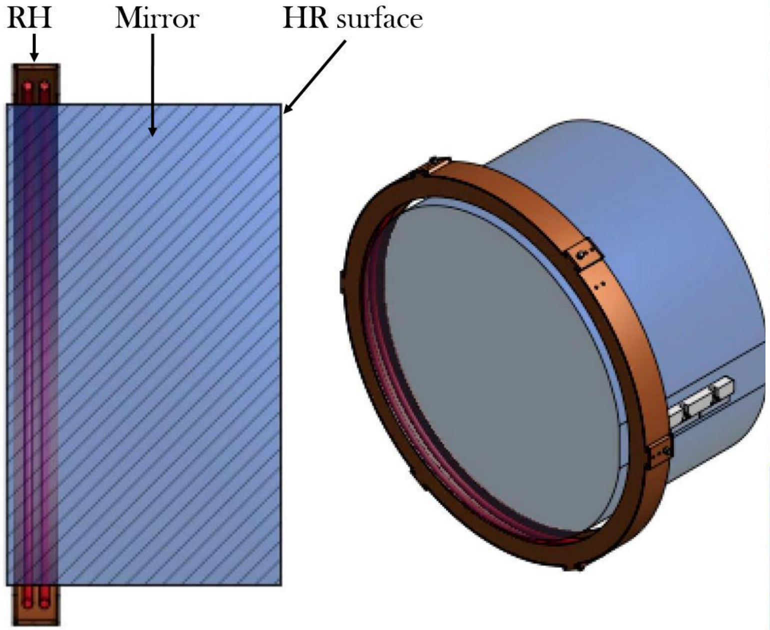

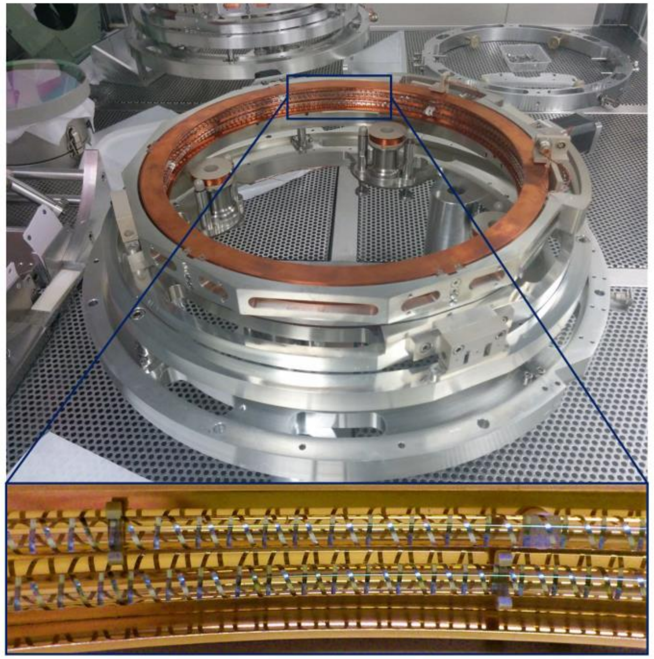

Compensation of the thermal lensing: CO_2 laser projectors

- The correction of thermal lensing caused by the thermo-optic effect is performed by heating the mirror, but through a method distinct from the one previously described.
- Thermal lensing arises primarily from the radial component of the temperature gradient. To counteract this, the compensation involves heating the periphery of the mirror, effectively cancelling out the temperature gradient within it.

Correction strategy

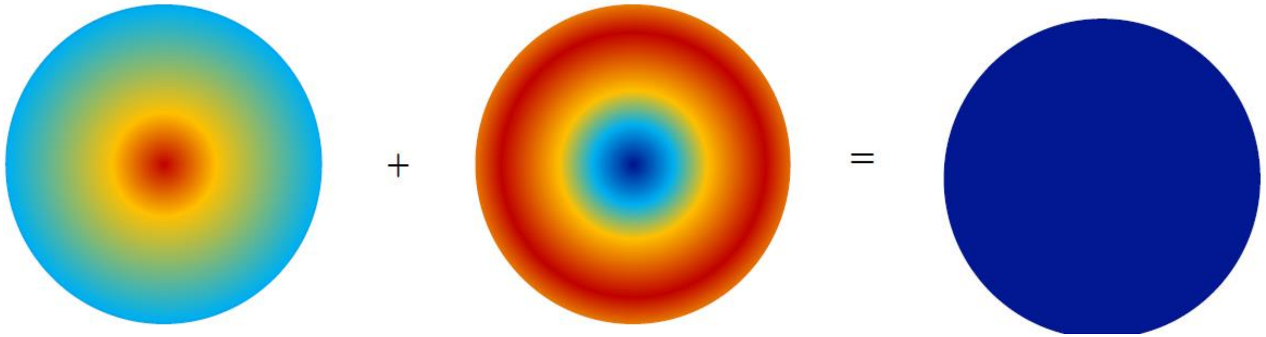

Mirror heated by the YAG main laser

Mirror heated by TCS actuator

Cold mirror

Compensation of the thermal lensing: CO_2 laser projectors

- A suitable approach for correcting thermal lensing is to shine on the optic a radiation which is completely absorbed in a thin surface layer. For mirrors made by fused silica, this requires the use of laser radiation with $\lambda > 5\ \mu m$ like **high-power CO_2 lasers** emitting at $\lambda = 10.6\ \mu m$.
- This wavelength allows the generation of a variety of heating profiles, from which the most suitable one can be selected.
- To minimize noise coupling between the laser and the optics, the CO_2 laser is not shined directly onto the mirror but instead onto an additional transmissive optic known as the Compensation Plate (CP). The CP enables independent control of both the thermal lensing compensation and the correction of the RoC.

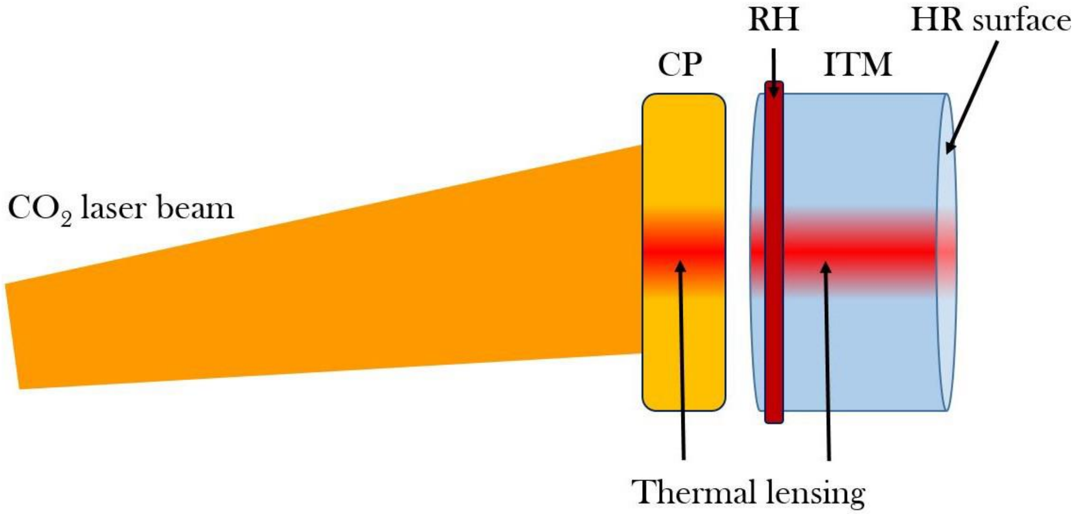

Projected patterns – Central Heating

- The actuation patterns projected on the CP are the **Central Heating (CH)** and the **Double Axicon System (DAS).**

- **CH** consist of a Gaussian beam shined at the centre of the CP with the same dimensions as the main YAG laser beam.

- This pattern generates a negative lens, with the same sign as the thermal lensing caused by the self-heating of the optics from the main YAG beam.

- Its purpose is to mitigate thermal transients when the interferometer loses the lock, helping the system to recover faster the correct working point.

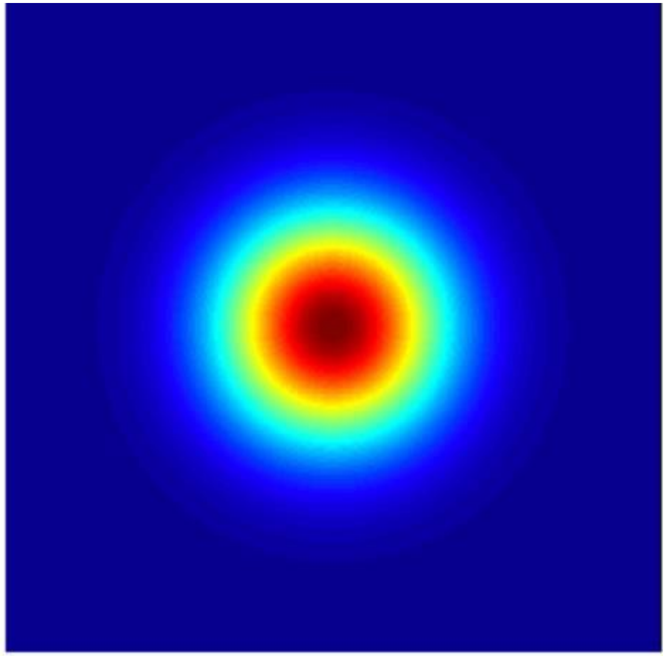

Projected patterns – Double Axicon System

- **DAS**, on the other hand, is created by superimposing two annular beams of different sizes and radii to form a donut-shaped profile.
- The annular patter is produced using an axicon - a lens with a conical surface that could convert a Gaussian laser beam into an annular one.
- Unlike the CH, the DAS generates a positive lens. It is used mainly to correct the thermal lensing due to uniform coating absorption in the ITMs and the cold defects showing a high degree of spherical aberration.

The best compensation is obtained by applying a profile that is the sum of two annuli:

- INNER annulus → thick and weak
- OUTER annulus → thin and bright

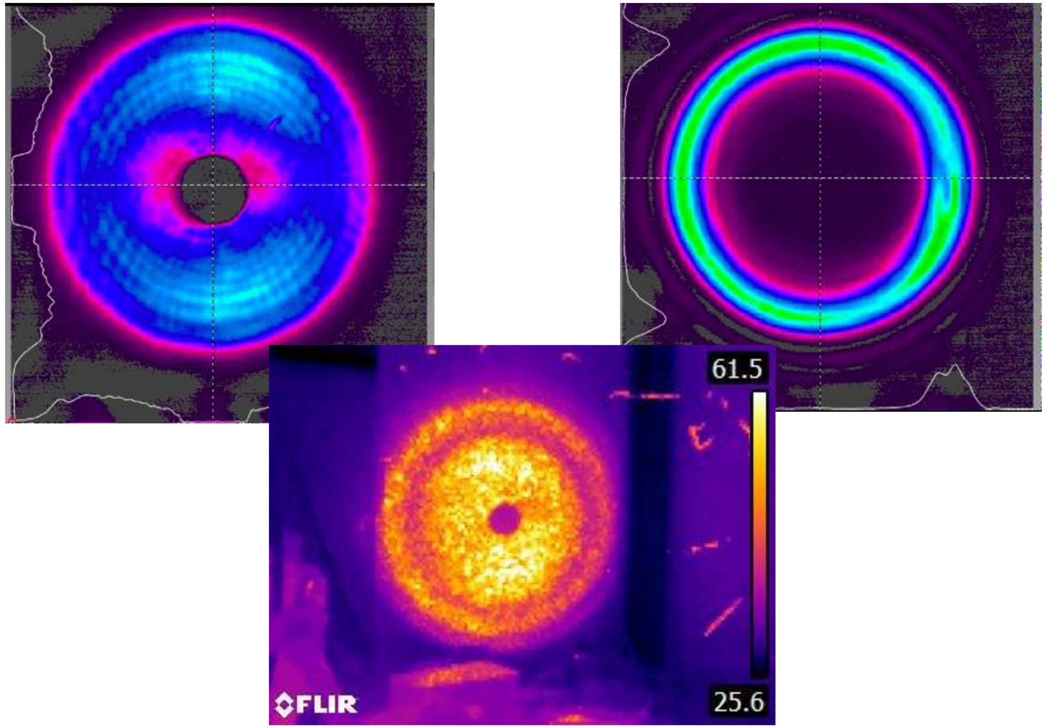

Actuators check – Projected patterns

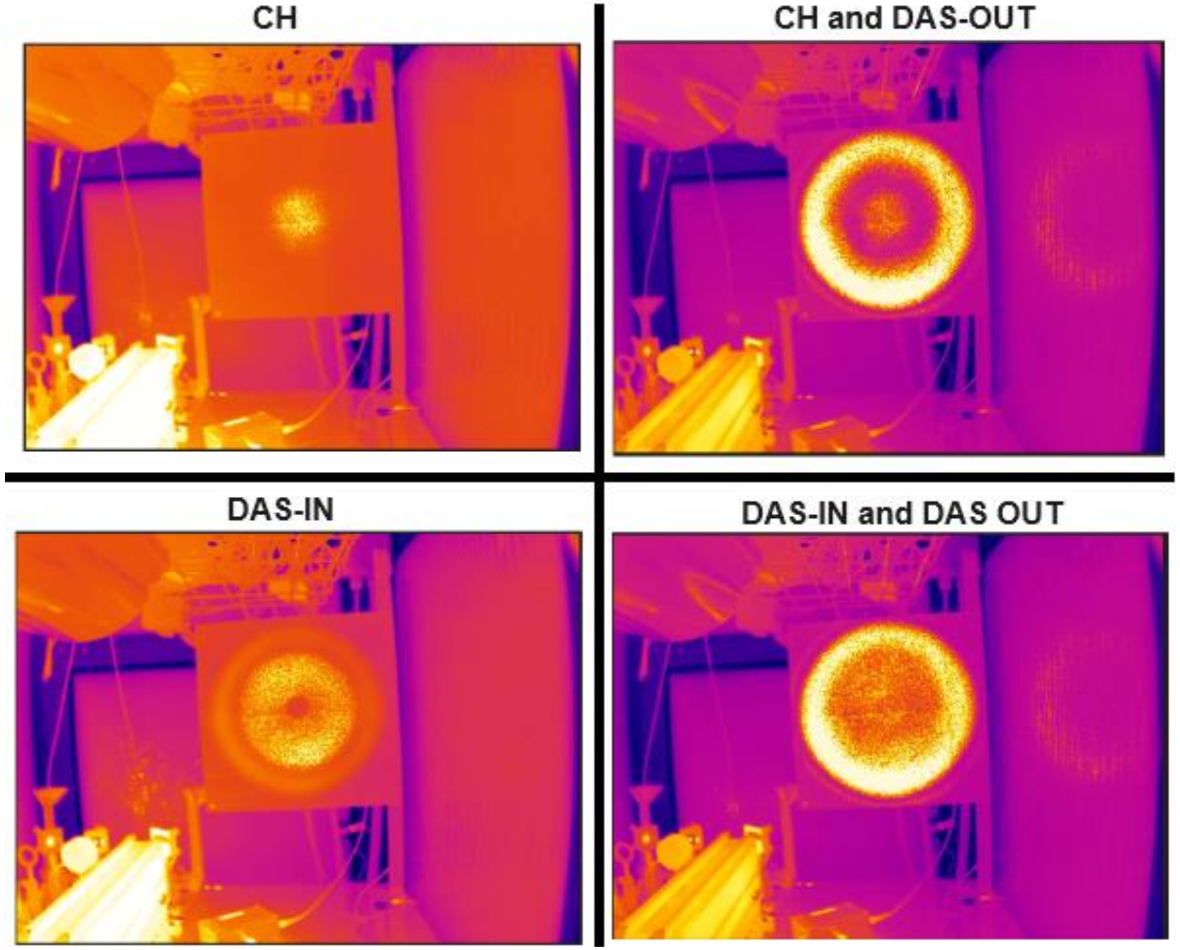

- Intensity distribution on a cardboard observed with a thermal camera

Sensors + actuators: the Thermal Compensation System

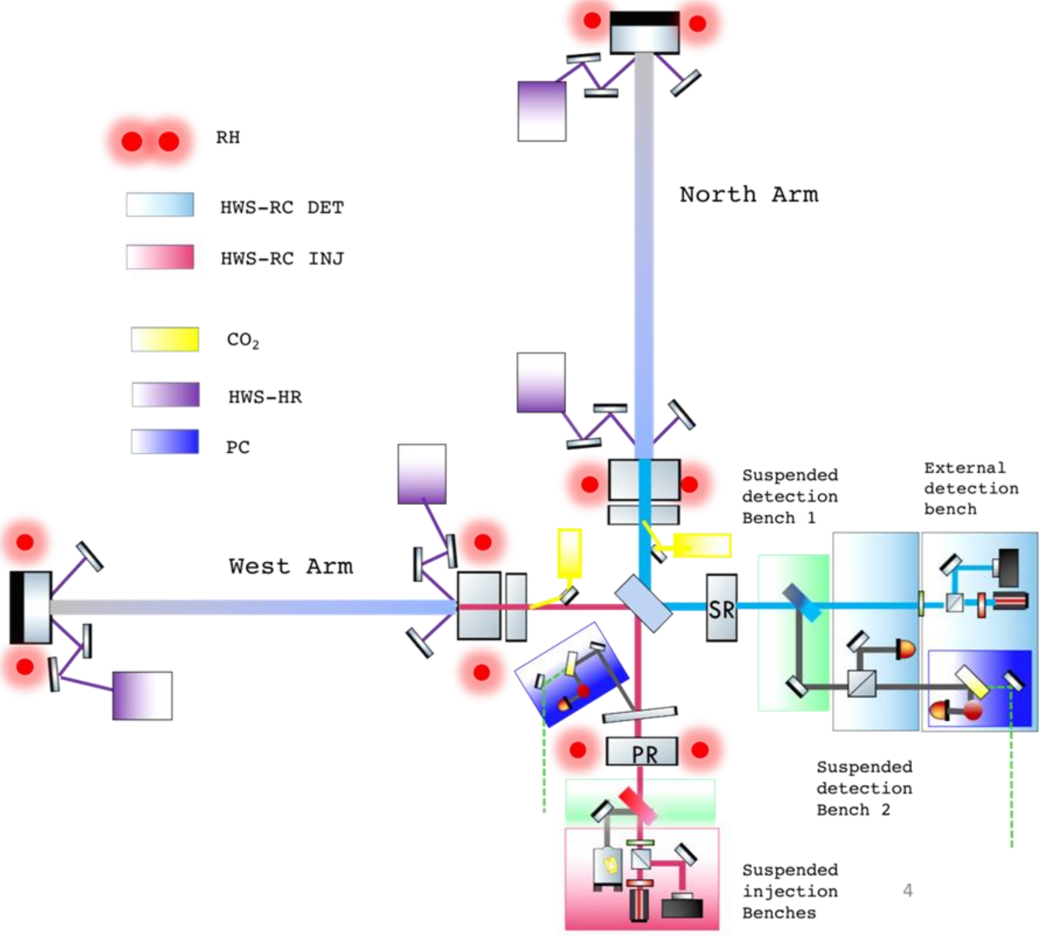

(Some) Current TCS' results so far

ITMs coating absorption measurements

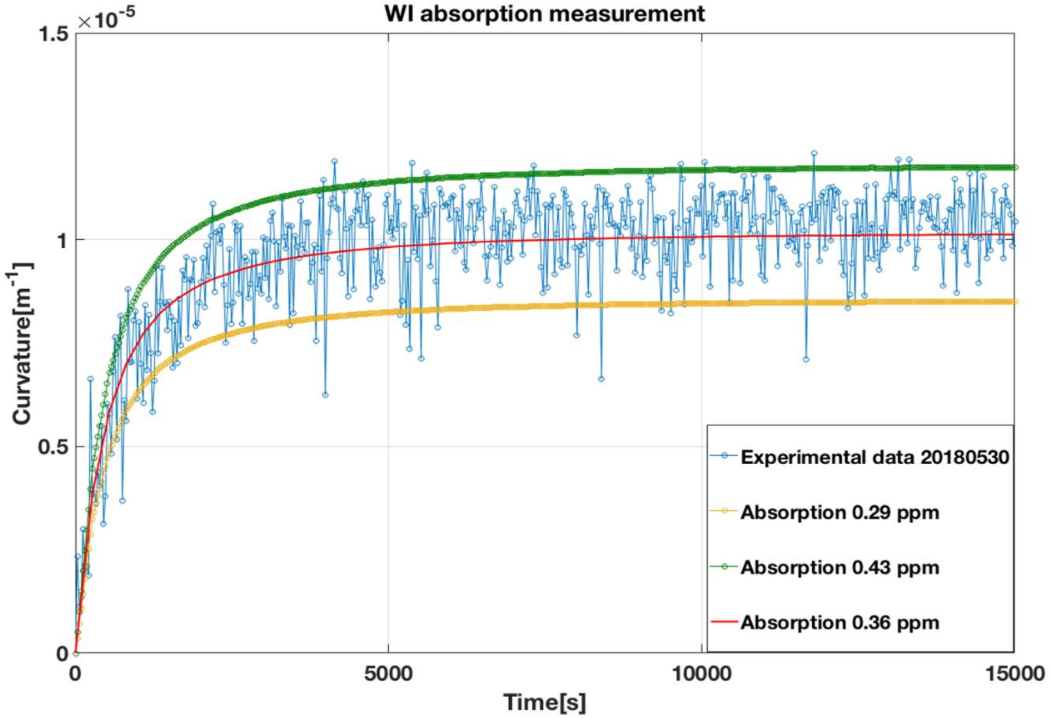

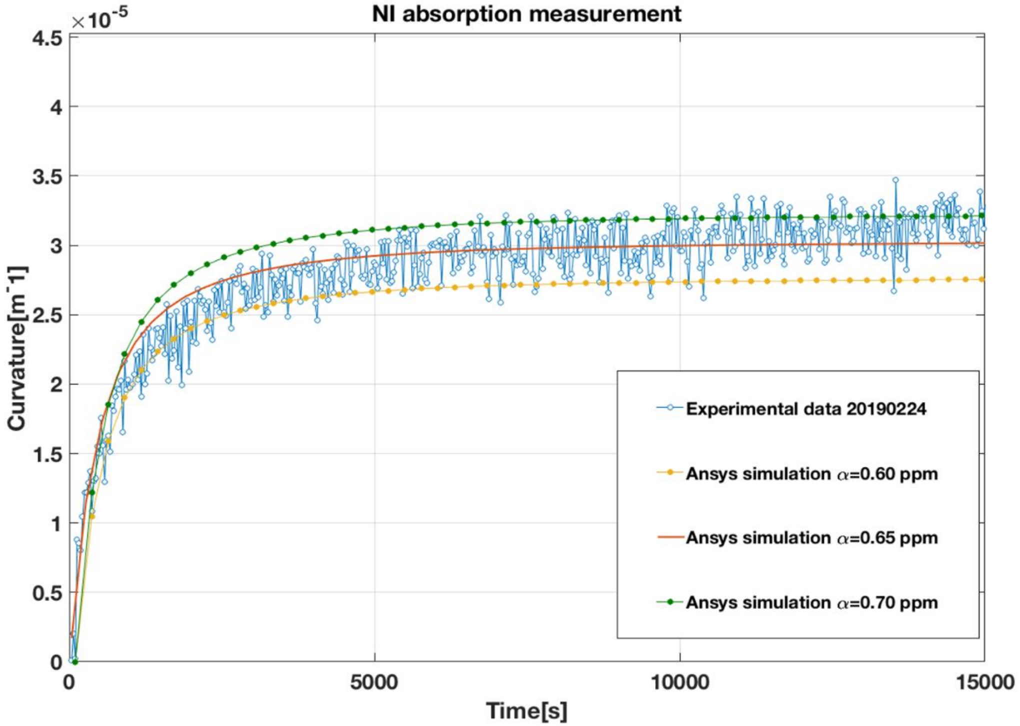

ITM	LMA	HWS (2018-19)	HWS (2023)
NI	(0.19±0.08) ppm	(0.65 ± 0.05) ppm	(0.60 ± 0.09) ppm
WI	(0.22±0.06) ppm	(0.36 ± 0.07) ppm	(0.29 ± 0.03) ppm

ETM RHs effect: intracavity power increase and darker fringe

- Optical power in the arms
- North arm: 455 mW → 535 mW.
- West arm: 435 mW → 520 mW.
- **Net increase of the intra-cavity power of about 15%**.

- Dark fringe
- Power detected at the dark port: 0.300 mW → 0.179 mW.
- **Improvement of around 68%.**

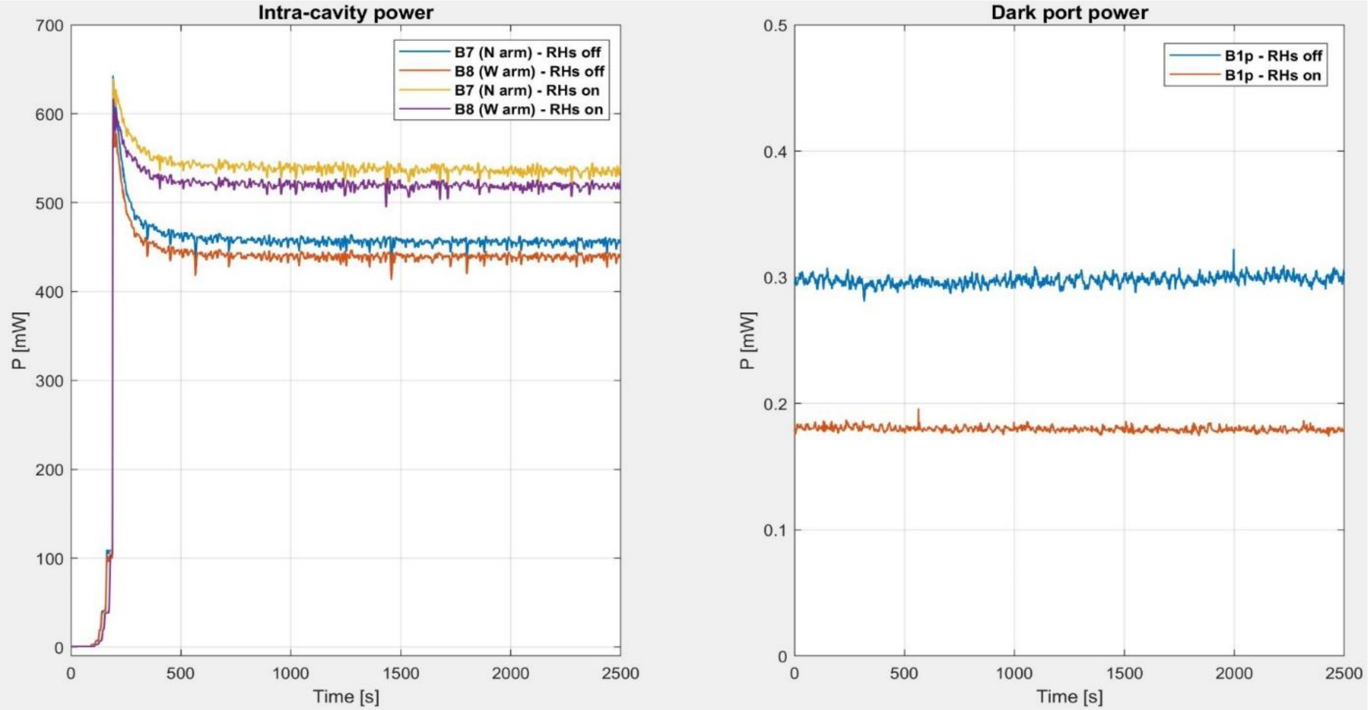

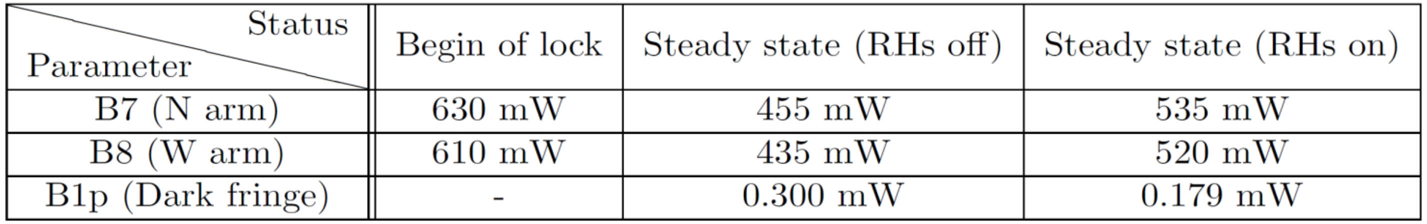

Status / Parameter	Begin of lock	Steady state (RHs off)	Steady state (RHs on)
B7 (N arm)	630 mW	455 mW	535 mW
B8 (W arm)	610 mW	435 mW	520 mW
B1p (Dark fringe)	-	0.300 mW	0.179 mW

Sensing and actuation validation

- Reference wavefront: interferometer not locked, DAS off.
- Begin of the measurement: interferometer reached the dark fringe. Curvature started to increase, due to the natural thermal lensing of the YAG laser.
- WI DAS shined: curvature on the related interferometer started to decrease toward the zero.
- Interferometer unlocked: the curvature sign changed as expected because the DAS was on but there were no more the YAG thermal lensing to balance it.
- Interferometer relocked (with the actuator still on): the curvature started to come back to zero.

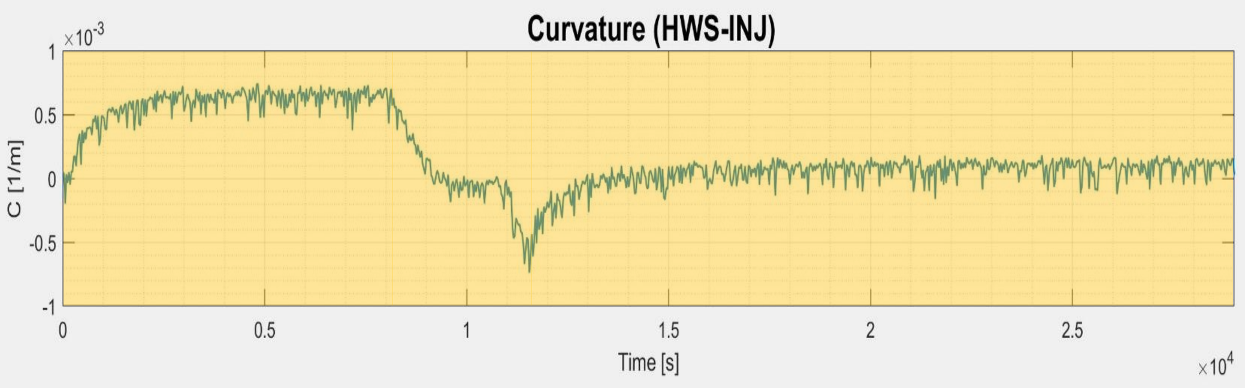

Improvements observed with the Phase Camera

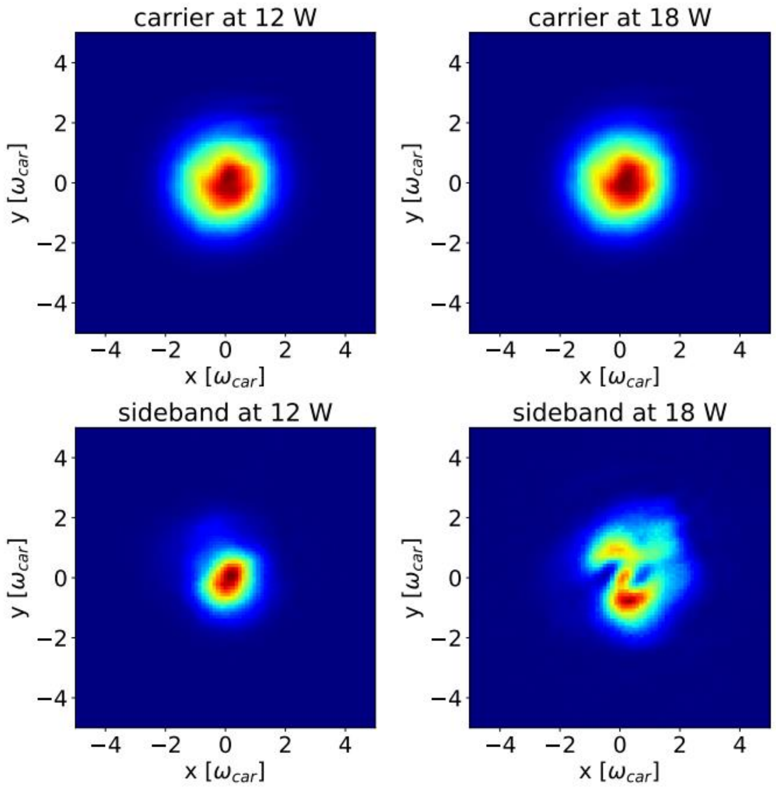

Effect of thermal effects on the intensity images without thermal compensation, measured with the PC.

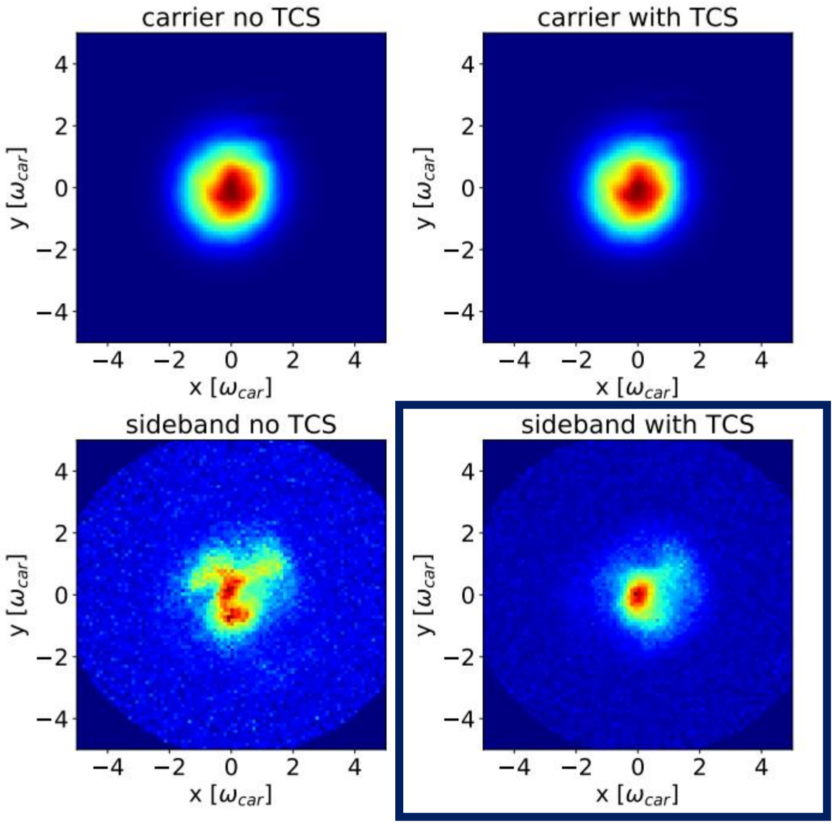

Effect of thermal effects on the intensity images for **24 W** laser power without and with TCS.

TCS impact on sensitivity curve

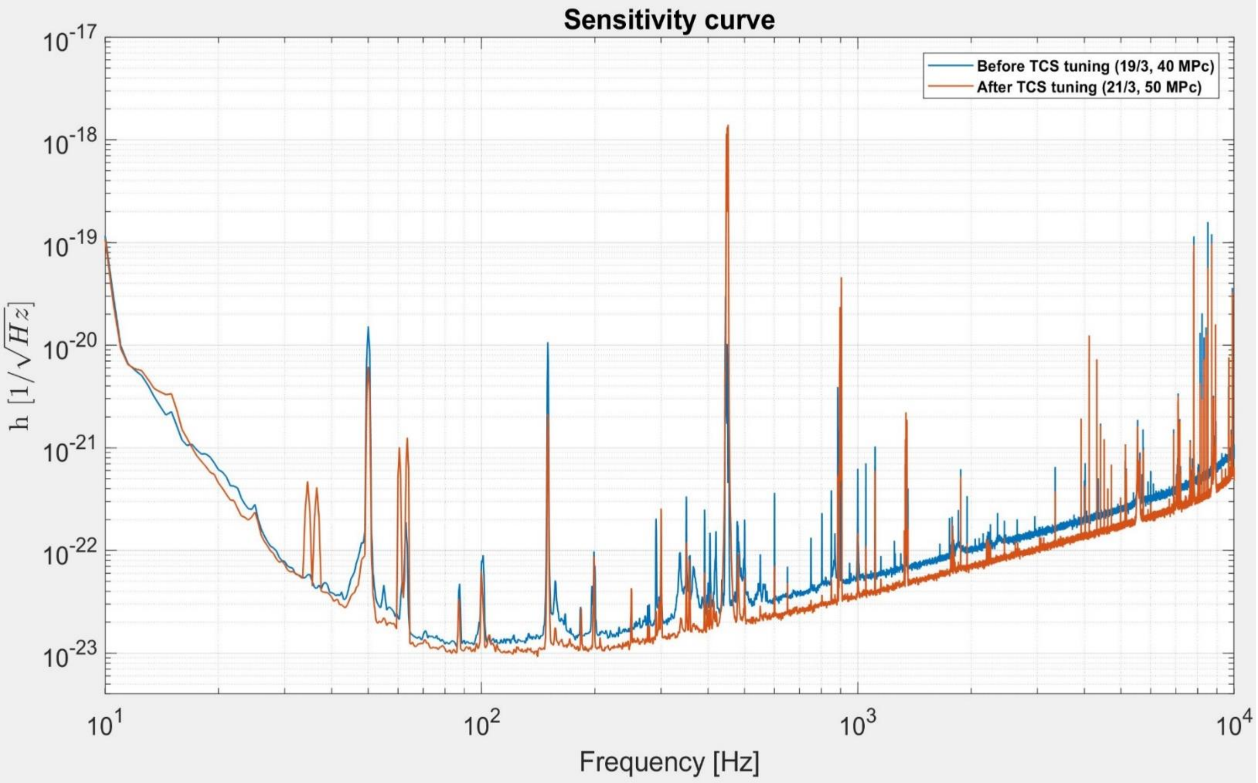

Commissioning for O3 (2019)

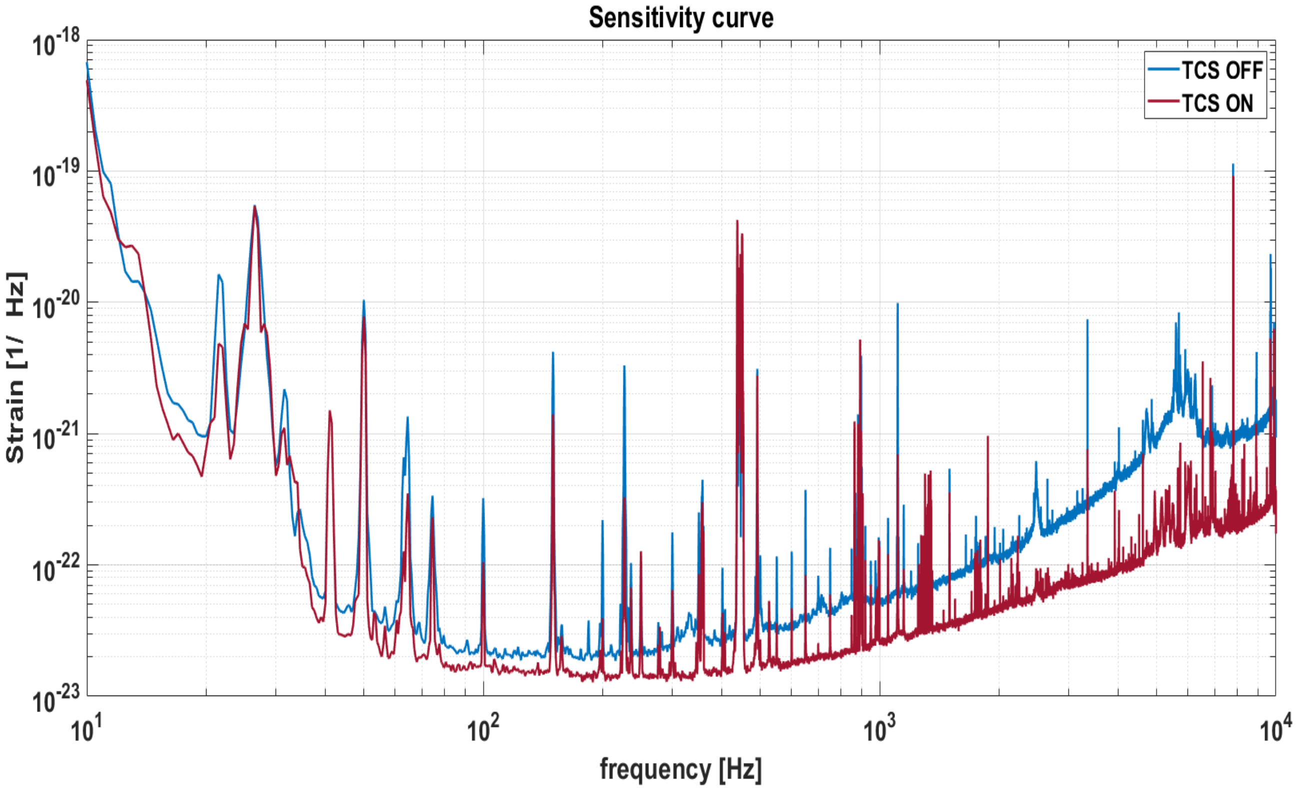

Commissioning for O4b (2024)

The (future) solution

Thermal Compensation System upgrades and R&Ds in view of ET-HF

Advanced optics laboratories for ET @ Rome Tor Vergata

AILOV ET

ADVANCED OPTICS LAB @ TOR VERGATA FOR ET

- Development of innovative technologies for sensing and control wavefront aberrations

- Creation of new facilities for **Aberration Control (WSC)**
- Development of techniques for the mitigation of the optical aberration in the optics of ET
- Study of new actuators and new sensors and of the correlation of the thermal effects with the control signals of an optical cavity

Sensing and testing thermal effects in the lab

- A new facility with a marginally-stable cavity (MSC) is foreseen to be installed and commissioned in the Virgo/ET Tor Vergata laboratories.
- This kind of cavity is very sensitive to optical aberrations: any small departure from the design parameters leads to a change in the cavity resonance conditions and in the degeneracy of its eigenmodes.
- As such, a MSC can be seen as an "amplifier" of wavefront distortions.

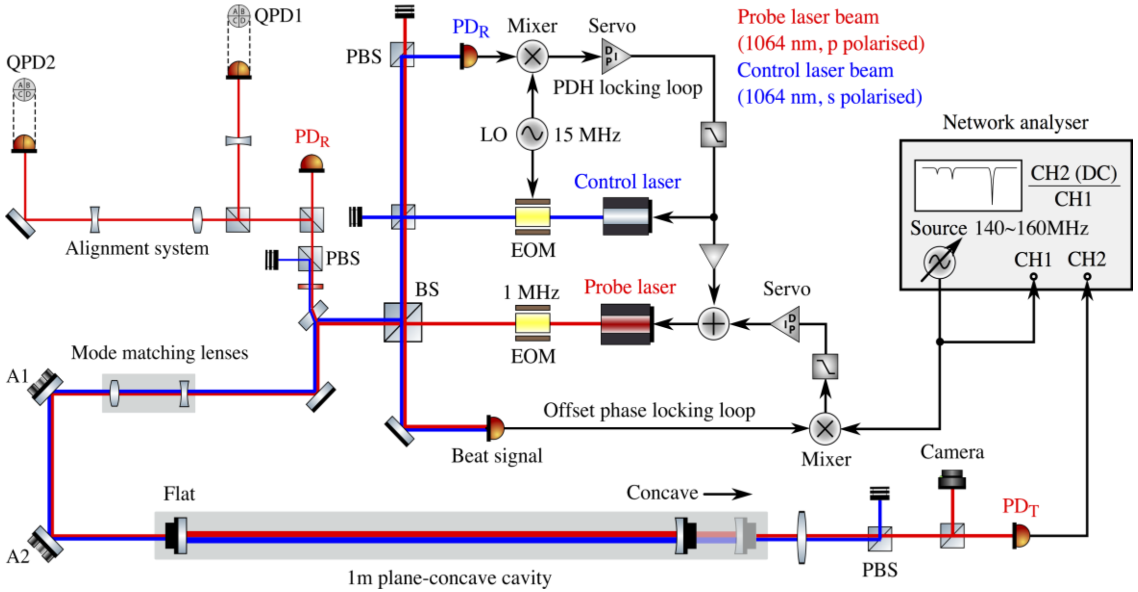

H. Wang et al., Phys. Rev. D 97, 022001 (2018)

New HWS sensor

- The **DALSA** Teledyne Company has put out of production the **Pantera 1M60 CCD** necessitating the search for an alternative solution.
- A new **CMOS-based Hartmann Wavefront Sensor** is currently under test, identified in collaboration with Adelaide University. So far, it proved similar performances with respect to Dalsa.
- **New custom thermal housing** in aluminum for the naked CMOS.
- Plate **temperature control** within ~40mK to keep thermal defocus below requirements.

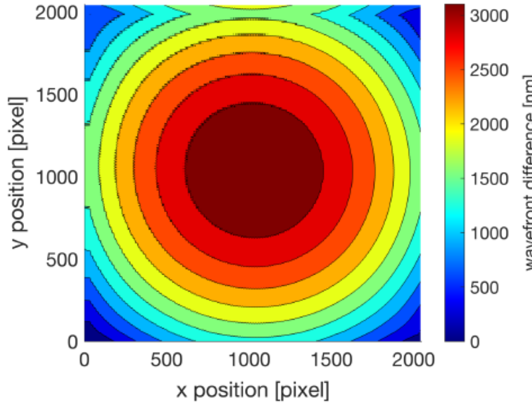

- CMOS sensor allows for:
  - Faster response;
  - Reduced power consumption;
  - Enhanced image processing functionalities;
  - Lower price.

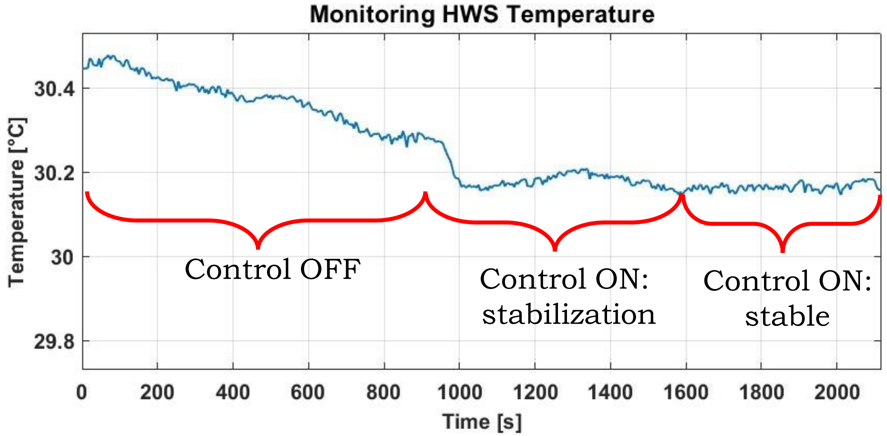

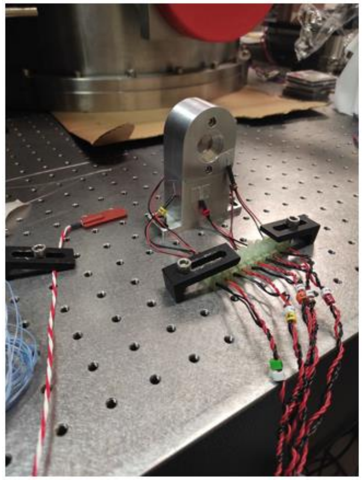

Adaptive Optics for non-axisymmetric aberrations correction

- Deformable mirror actuator with high stability to be implemented in MSC facility for the correction of non-axisimmetric aberrations.
- ALPAO DM:
- 97 electro-magnetic actuators
- Pupil diameter: 13.5 mm

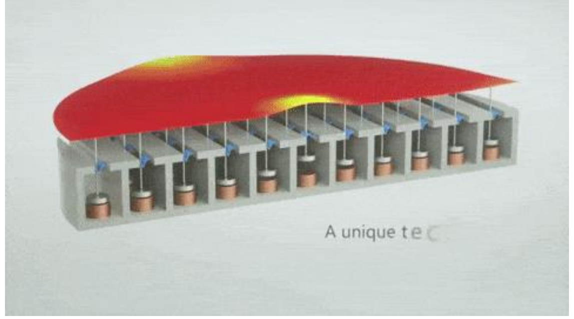

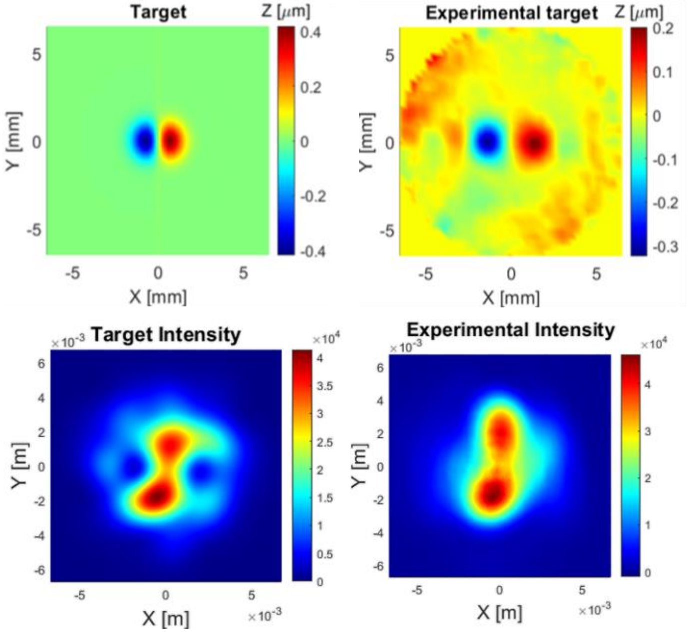

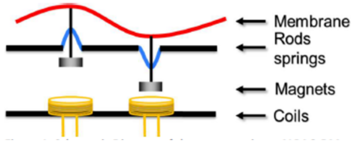

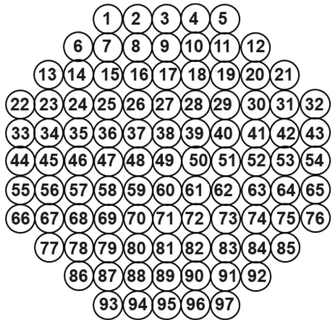

Current status:

- ALPAO DM characterized
- Good agreement with target pattern in terms of phase and intensity
- A new ALPAO DM with 192 actuators has been purchased
- Preliminary check of its actuators performed in late October 2024

Credit: C. Taranto

DAS improvements

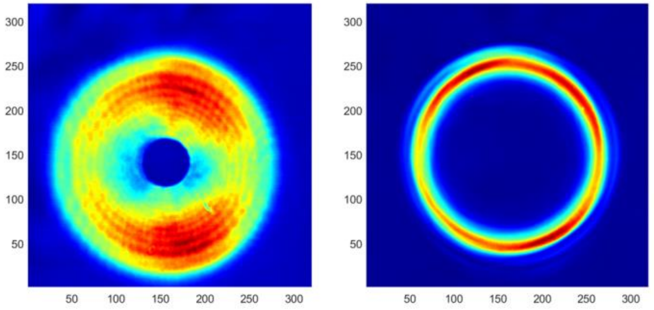

Inner and outer DAS measured intensity

- Imperfections in the DAS intensity profile are traced back to:
  - Presence of Higher Order Modes in the CO_2 laser beam;
  - Specific features of the current optical layout.

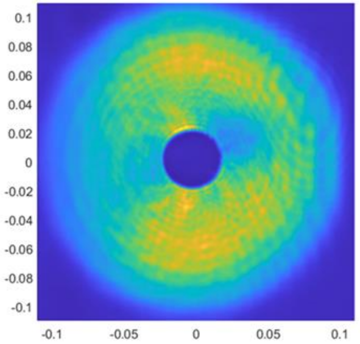

Measurement

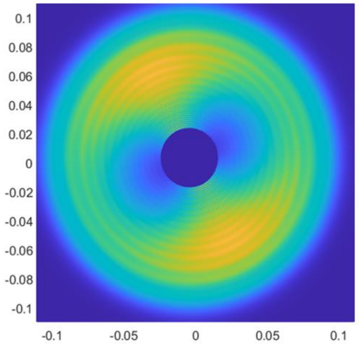

FFT simulation with astigmatic input beam

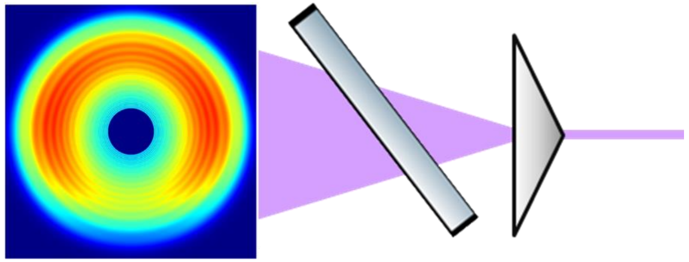

Left-Right asymmetry due to beam angle of incidence on partially reflecting optics

DAS improvements – Angle of incidence

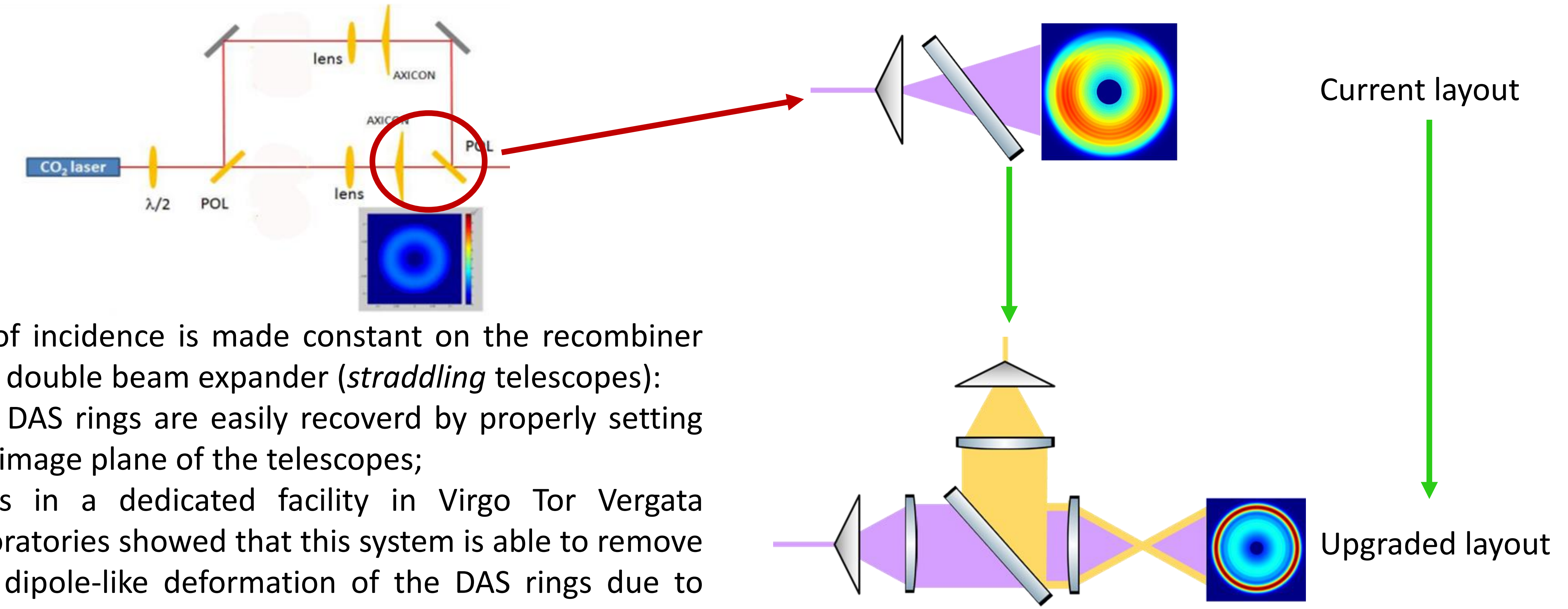

Angle of incidence is made constant on the recombiner using a double beam expander (*straddling* telescopes):

- The DAS rings are easily recoverd by properly setting the image plane of the telescopes;
- Tests in a dedicated facility in Virgo Tor Vergata laboratories showed that this system is able to remove the dipole-like deformation of the DAS rings due to the effect of the angle of incidence.

DAS improvements – Quality of the beam/actuation improvement

- HOMs content in a TCS CO_2 source (Access 50W) is of the order of few percent
- Spatial filtering with a pinhole causes a drop of available power (50%!) and cannot totally remove HOMs
- Beam throughput - when HOMs are removed - is required to be >85% of input power

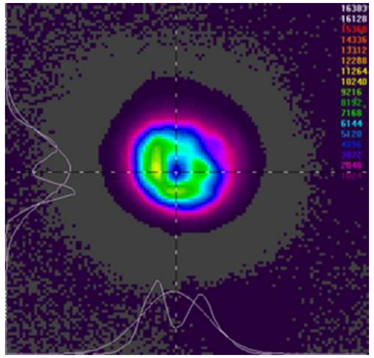

The best strategy is represented by a **mode cleaner cavity**:

- Triangular configuration (to avoid back-propagation when lacking Faraday isolators for CO_2)
- EOM is very expensive for CO_2 wavelength
- Dithering lock is the designed solution
- Invar case to avoid large drift due to high power buildup
- **Finesse 100, input source 50 W**!

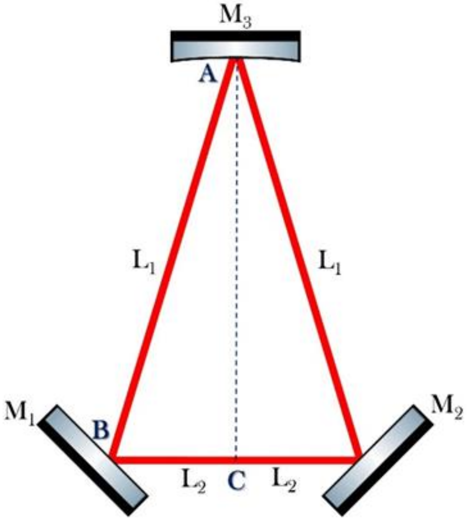

DAS improvements – Quality of the beam/actuation improvement

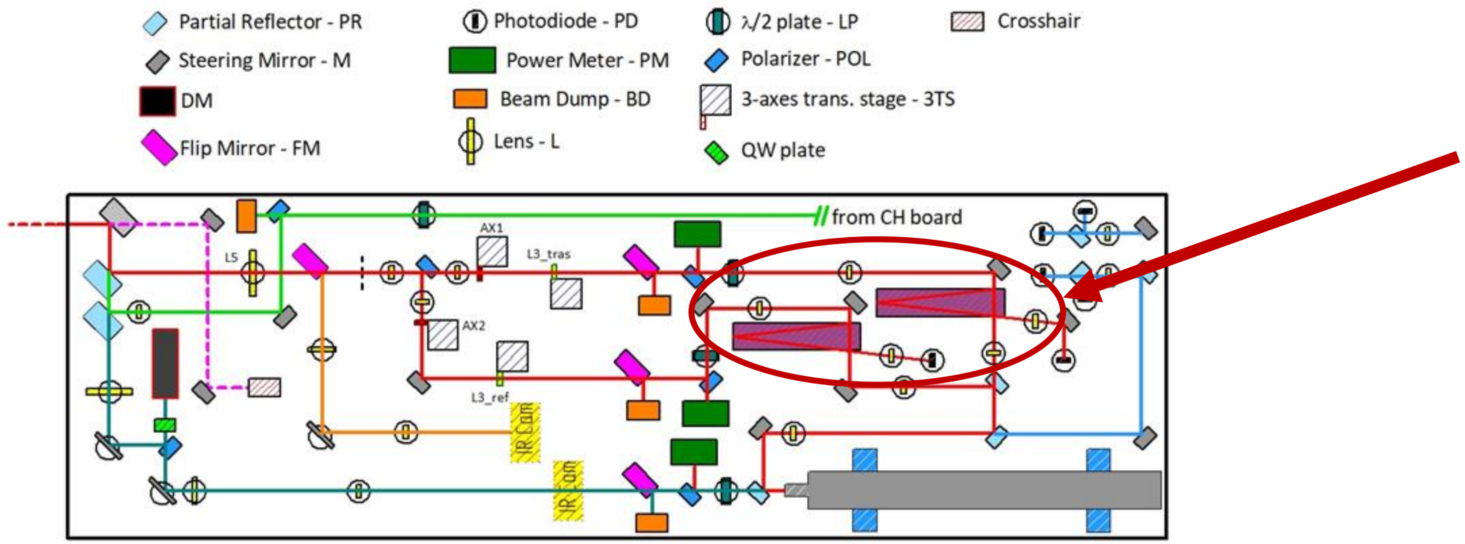

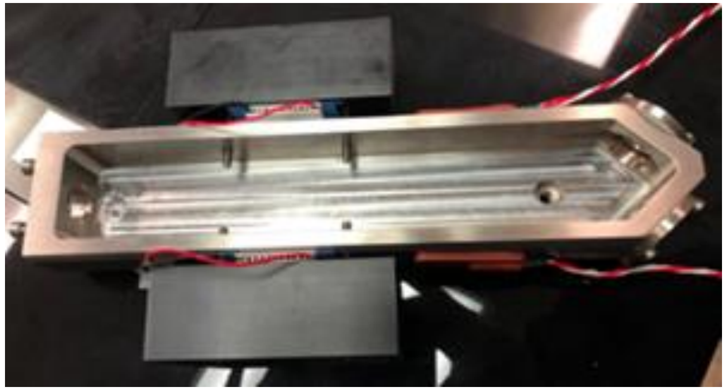

A prototype version of the MC is being develped at ToV

- Invar cavity spacer controlled in temperature with Peltier cells (stability at the 1 mK level RMS)
- ZnSe mirrors with low absorption (1/1000) measured with HWS
- Phase noise of CO$_2$ source (50W CCW from Access) characterized with a Mach-Zender setup
- Dither locking strategy using a piezo actuator on the curved mirror.

Point Absorbers

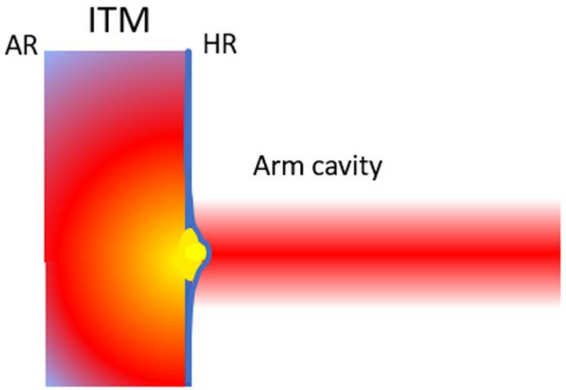

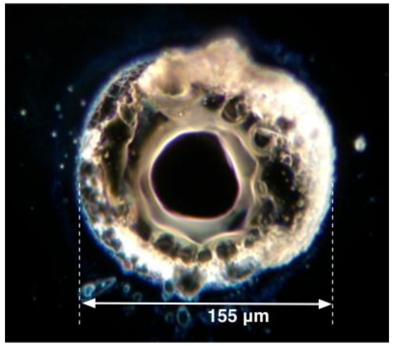

- Discovered during the O3 observing run on both LIGO and Virgo mirror after the increase of the laser input power

Characteristics:

- Localized small
- Randomly present on the High-Reflectivity mirror surfaces
- Highly absorbing
- Embedded in the coating
- Can not be cleaned
- Composition of high concentration of Aluminium

Effects of their presence:

- Scattering into Higher Order Modes
- Increase of optical losses
- Limits interferometer sensitivity

Point Absorbers behaviour and mitigation

- In November 2022, after a deep cleaning procedure, the WI points disappeared
- In May 2023, some points appeared in different positions

Actuator type: binary matrix with 40x40 actuators

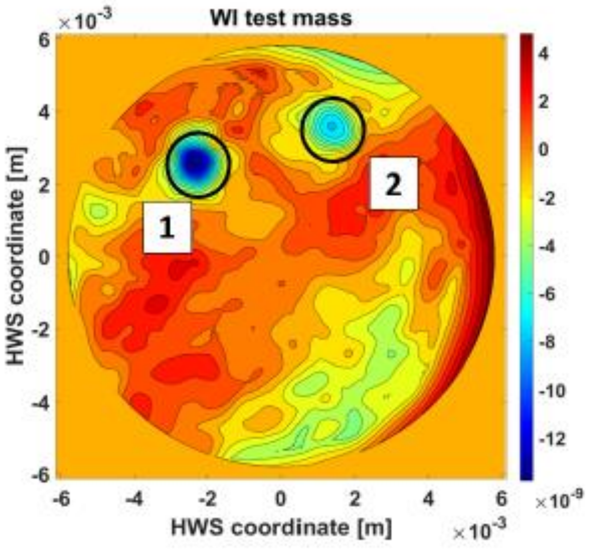

2018

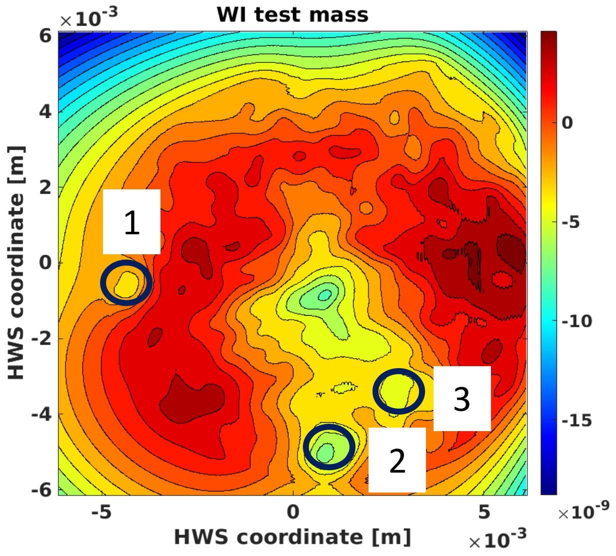

2023

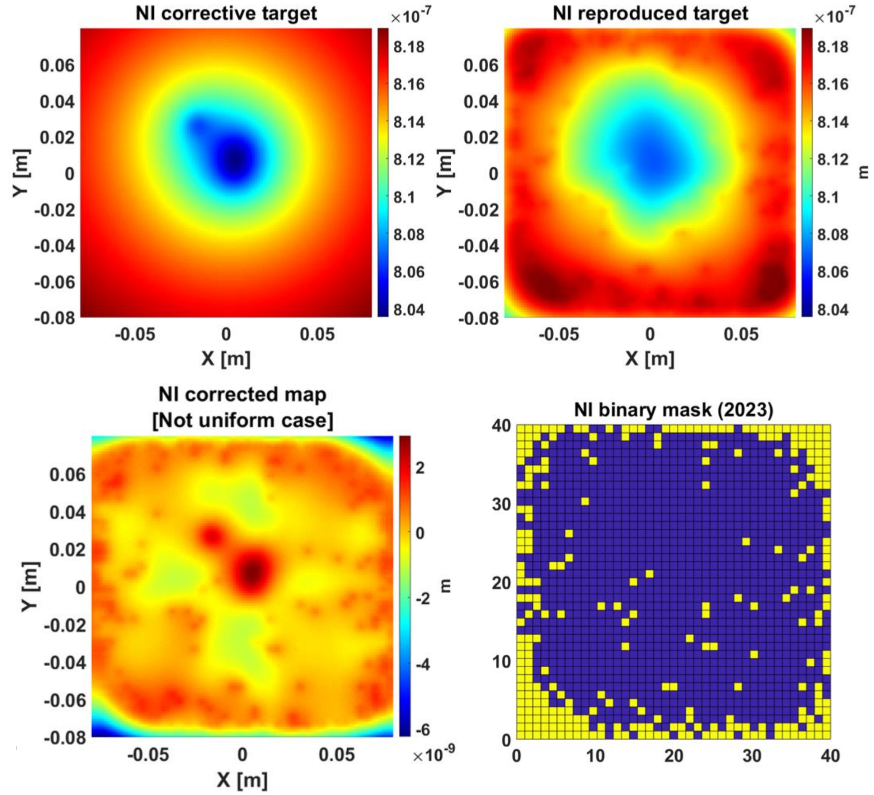

Point Absorbers mitigation

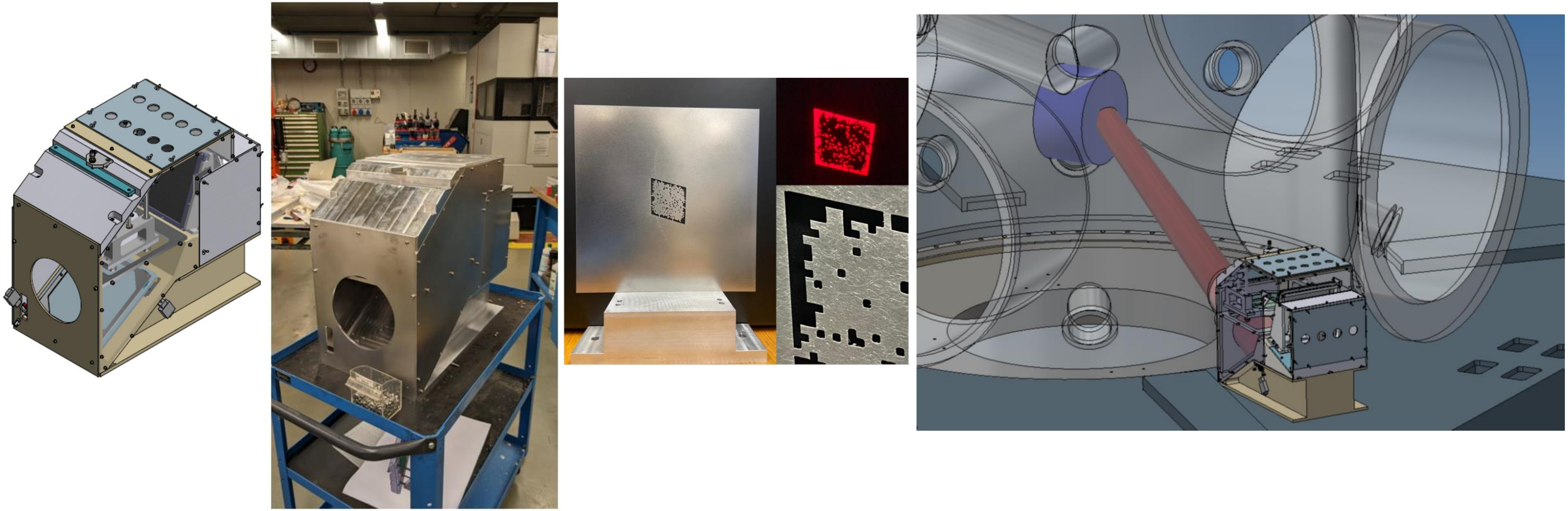

What about ET-LF?

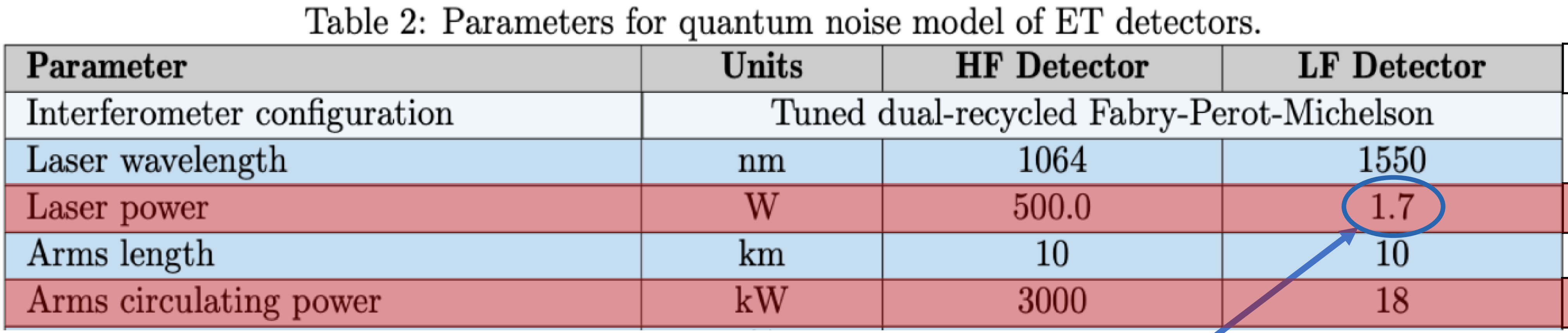

Table 2: Parameters for quantum noise model of ET detectors.

Parameter	Units	HF Detector	LF Detector	Current Advanced Virgo +
Interferometer configuration	Tuned dual-recycled Fabry-Perot-Michelson			
Laser wavelength	nm	1064	1550	
Laser power	W	500.0	1.7	18 W
Arms length	km	10	10	
Arms circulating power	kW	3000	18	~100 kW

For comparison, Advanced Virgo joined O2 with 10 W of input power and TCS off.

Conclusions

- The quantum shot noise limits the high-frequency part of the GW detectors
- It can be corrected by increasing the laser input (and circulating) power, at the expense of increasing the thermal effects as well
- The optical aberrations which are generated can strongly limit the stability and the correct operation of the interferometer
- A dedicated subsystem – the TCS – is devoted to monitoring and tackling optical aberrations
- So far, TCS demonstrated to be crucial to ensure the correct working point of the detector…
- … but for next-generation GW – like ET-HF – an upgrade of it is necessary, with the development of new more efficient and versatile sensing and actuations systems

Thank you for your attention!

Contact: lorenzo.aiello@roma2.infn.it

Backup slides

Quantum shot noise

- Laser light comes in discrete quanta (photons)
- Given an observation time T and a number of photon N_γ, the average power measured by a photodetector is given by

$$P = \frac{N_\gamma \hbar \omega_L}{T}$$

- The distribution of the counting of a number of discrete independent event is a Poisson one
- Large N: Poisson distribution → Gaussian distribution with S.D.=$\sqrt{N}$ (Central Limit Theorem)
- Fluctuations in n° of photons $\Delta N_\gamma = \sqrt{N_\gamma}$ → $\Delta P_{shot} = \sqrt{\frac{\hbar \omega_L P}{T}}$

Quantum noise and the Standard Quantum Limit

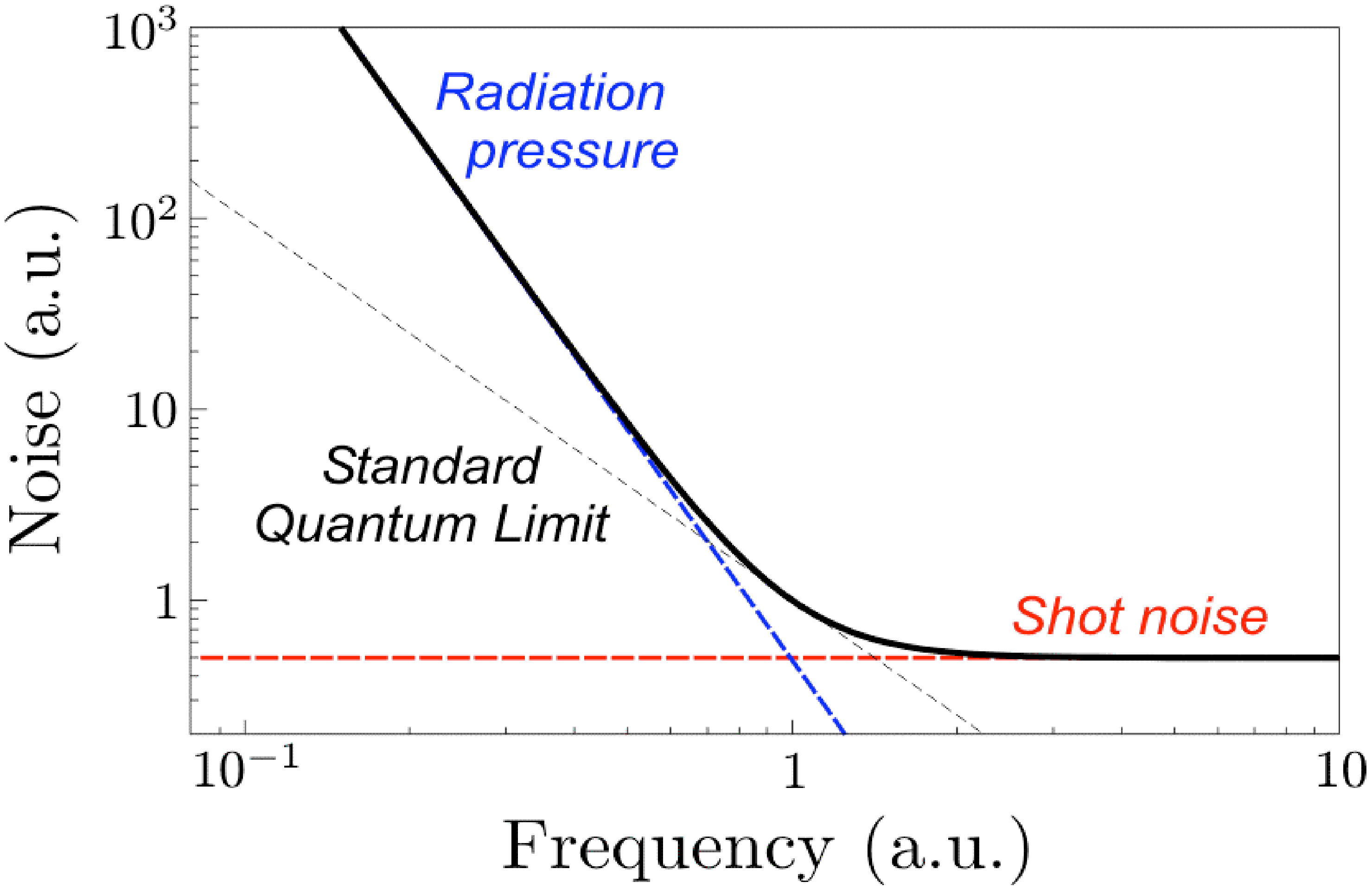

Actuators alignment check in HWS maps

	Ring Heater	Central Heating	Double Axicon System
WI mirror	WI RH (HWS-INJ MAP)	WI CH (HWS-INJ MAP)	WI DAS (HWS-INJ MAP)
NI mirror	NI RH (HWS-DET MAP)	NI CH (HWS-DET MAP)	NI DAS (HWS-DET MAP)

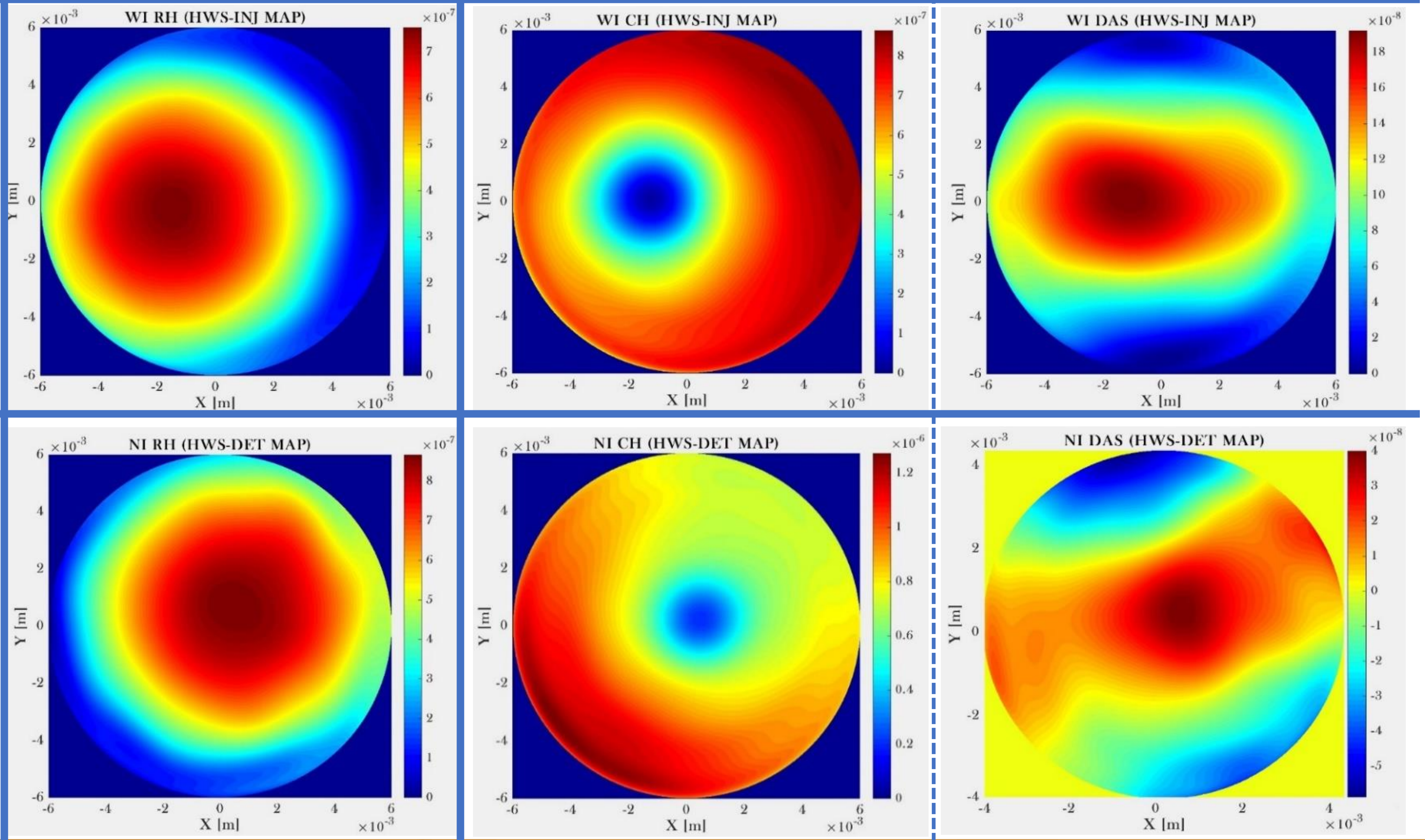

Astigmatism

- **Astigmatism** is an optical aberration that occurs when rays lying in two perpendicular planes on the optical axis have different foci.
- This causes blur in one direction that is absent in the other direction. If we focus the sensor for the sagittal plane, we see circles become ellipses in the tangential direction and vice versa.
- If an optical system with astigmatism is used to form an image of a cross, the vertical and horizontal lines will be in sharp focus at two different distances.

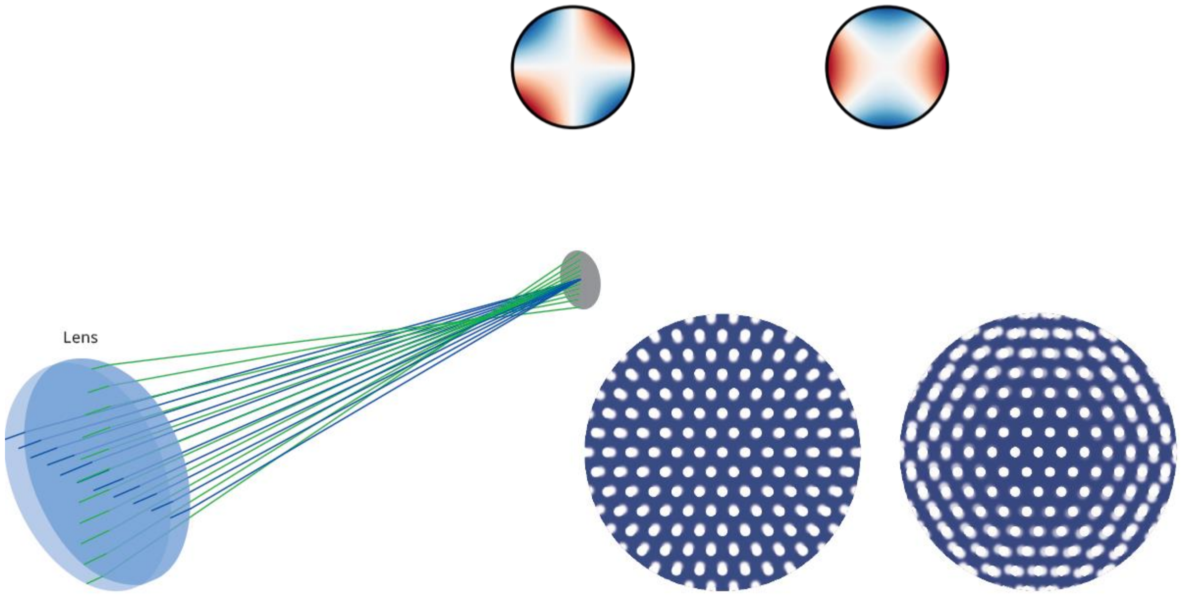

DAS effect: Power recycling cavity gain improvement

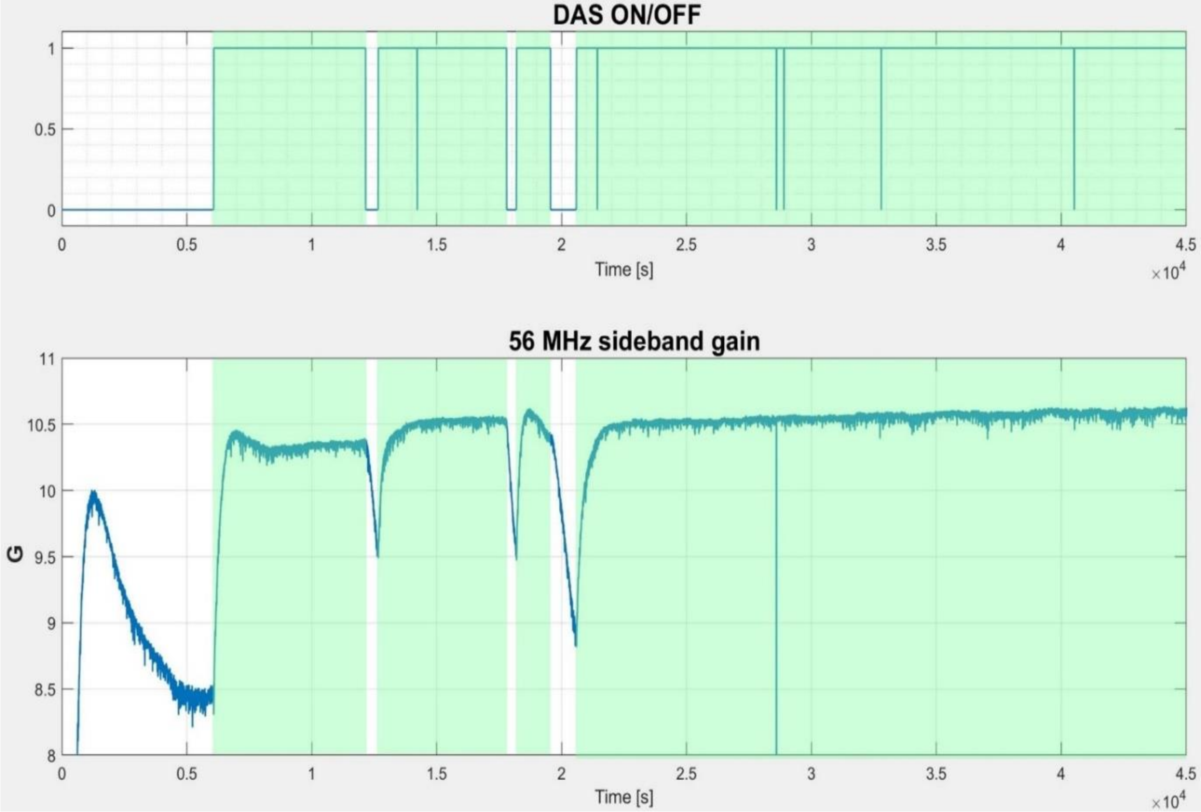

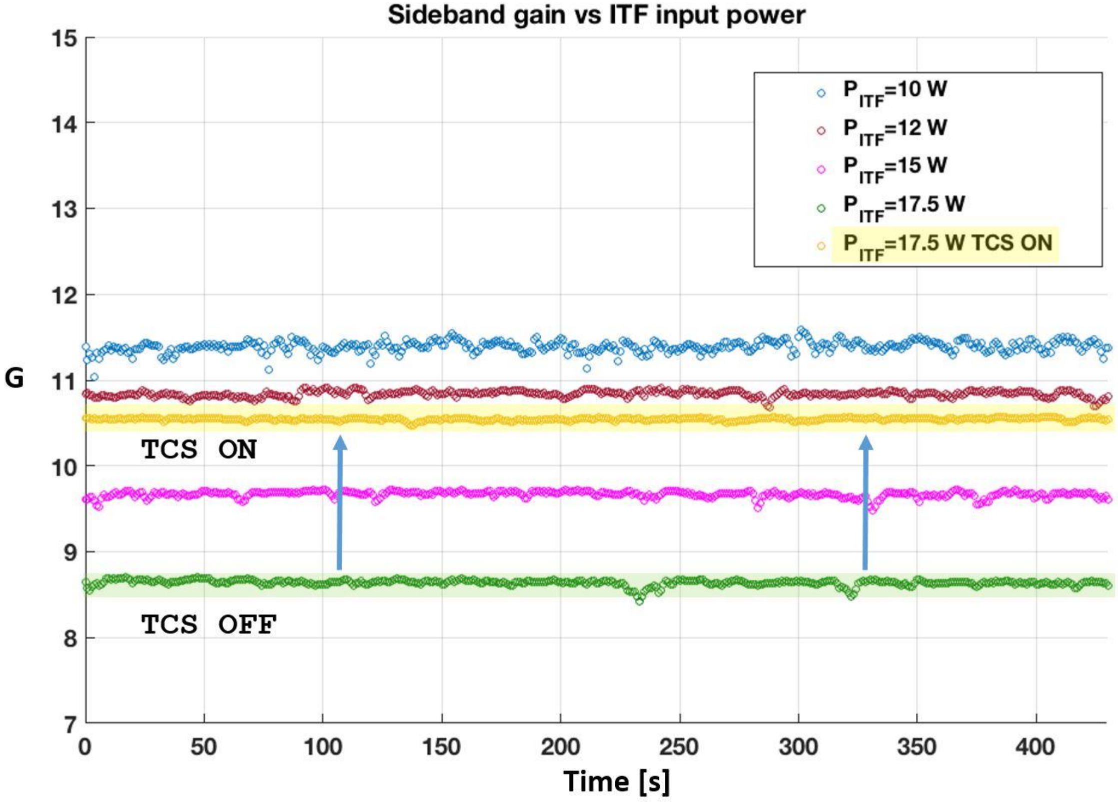

Point Absorbers mitigation